Title
The rarity of terrestrial gamma-ray flashes: 2. RHESSI stacking analysis

Journal
Journal of Geophysical Research: Atmospheres, 121(19)

ISSN
2169-897X

Authors
Smith, DM
Buzbee, P
Kelley, NA
et al.

Publication Date
2016-10-16

DOI
10.1002/2016jd025395

Peer reviewed

The rarity of terrestrial gamma-ray flashes II: *RHESSI* stacking analysis

D. M. Smith,[1] P. Buzbee,[1,2] N. A. Kelley,[1,3] A. Infanger,[1] R. H. Holzworth,[4]

and J. R. Dwyer[5]

D. M. Smith, Physics Department and Santa Cruz Institute for Particle Physics, University of California, Santa Cruz, 1156 High St., Santa Cruz, CA 95064, USA. (dsmith@scipp.ucsc.edu)

[1]Santa Cruz Institute for Particle Physics

Abstract.

We searched for gamma-ray emission from lightning using the *Reuven Ramaty High Energy Solar Spectroscopic Imager (RHESSI)* satellite by identifying times when *RHESSI* was near over 2 million lightning discharges localized by the Worldwide Lightning Location Network (WWLLN). We then stacked together the gamma-ray arrival times relative to the sferic times, correcting for light propagation time to the satellite. The resulting stacked gamma-ray time profile is sensitive to an average level of gamma-ray emission per

and Physics Department, University of California, Santa Cruz, Santa Cruz, California, USA.

[2]Google Inc., Mountain View, California, USA.

[3]Berkeley Applied Analytics, Berkeley, California, USA.

[4]Department of Earth and Space Sciences, University of Washington, Seattle, Washington, USA.

[5]Institute for the Study of Earth, Oceans, and Space, University of New Hampshire, Durham, New Hampshire, USA.

lightning discharge far lower than what can be recognized above background for a single Terrestrial Gamma-ray Flash (TGF). The summed signal from presumed small, previously unknown TGFs simultaneous with WWLLN discharges is remarkably weak: for the region from 0–300 km beneath *RHESSI*'s footprint, $(6.2 \pm 3.8) \times 10^{-3}$ detector counts/discharge are measured, as opposed to a typical range of 12–50 detector counts for TGFs identified solely from the gamma-ray signal. Under the assumption of a broken power-law differential distribution of TGF intensities, we find that the index must harden dramatically or cut off just below the sensitivity limit of current satellites, and that for most scenarios less than 1% of lightning can produce a TGF that belongs anywhere in the same distribution as those that are observable. For the minority of scenarios where more than a few percent of flashes produce a TGF, most of these "TGFs" are less than 10^{-4} of the luminosity of the faintest *RHESSI* TGFs, and therefore closer to the luminosity of lightning stepped leaders. The rarity of TGFs holds not only for TGFs simultaneous with the sferic observed by WWLLN, but for any time within 10 ms of the sferic, allowing (for example) for the possibility that different events within the upward propagation of a negative leader in positive intracloud lightning triggered the TGF and WWLLN's detection.

1. Introduction

The terrestrial gamma-ray flashes (TGFs) detected from low Earth orbit in association with thunderstorms are thought to involve on the order of 10^{17} or 10^{18} relativistic electrons, producing a comparable number of gamma-rays [*Dwyer and Smith*, 2005; *Carlson et al.*, 2007; *Gjesteland et al.*, 2015]. While containing significantly less total energy than the currents of ordinary lightning, these flashes are extraordinarily bright from the standpoint of gamma radiation detection, saturating the responses of orbiting detectors even at a distance of $\geq$ 600 km from the storm [*Grefenstette et al.*, 2007, 2009; *Gjesteland et al.*, 2010; *Tierney et al.*, 2013]. It has been pointed out [*Dwyer et al.*, 2010] that inside the production region of the TGF itself, radiation levels could be high enough to cause a health risk to anyone on an aircraft.

Those individual lightning discharges that have been both tied unequivocally to TGFs and categorized via well-studied VLF emissions have been classified as positive intracloud (+IC) events [*Cummer et al.*, 2005; *Stanley et al.*, 2006; *Shao et al.*, 2010; *Lu et al.*, 2010; *Lu et al.*, 2011], and most recently it has been shown that the TGF appears as a distinctive radio signature during the upward propagation of a leader from the main negative to upper positive charge center [*Cummer et al.*, 2011; *Dwyer and Cummer*, 2013; *Cummer et al.*, 2014, 2015; *Lyu et al.*, 2015]. Only a small fraction of lightning (much less than 1%) is creating TGFs that can be observed from space by current instruments [*Fuschino et al.*, 2011; *Østgaard et al.*, 2012; *Briggs et al.*, 2013; *Tierney et al.*, 2013]. But because TGFs are extremely brief (peaking from 100-500 μs in duration, with just a few lasting tens of microseconds or over one millisecond [*Briggs et al.*, 2013; *Marisaldi et al.*, 2015]), there are typically only one or two orders of magnitude of dynamic range between events that are barely detectable above background from satellites and those that begin to show saturation effects (high detector deadtime). How many fainter events remain to be discovered is an open question, and the main subject of this paper.

There is only one line of published evidence on the question that is not based on data taken from orbit. The Airborne Detector for Energetic Lightning Emissions (ADELE), flying near 14 km over the southeastern United States, passed within 4 km horizontal distance of 133 lightning flashes with no gamma-ray detections [*Smith et al.*, 2011]. We used these null results to set an upper limit of $\sim 1\%$ of the canonical luminosity of a TGF seen from space or less for each of these 133 flashes, for production altitudes of 8–16 km. *Østgaard et al.* [2012] combined ADELE's detection rate (1/1213 flashes within 10 km, and 0/133 flashes within 4 km) with a cutoff powerlaw distribution derived from *RHESSI* and *Fermi* data to suggest that approximately 2% of lightning produces a TGF somewhere in the distribution, noting also that a distribution that flattens out at low luminosity could give a TGF yield of up to 100% of lightning with TGFs occurring down to about 10^{12} relativistic electrons. *Hansen et al.* [2013] performed a second set of simulations that gave a different estimate for ADELE's sensitivity, suggesting that those limits should be weaker by about an order of magnitude, but even under that assumption they represent significant limits on TGF production at low altitude that could not be obtained from space.

The distribution of TGF intensities observed from space was suggested by *Collier et al.* [2011] to be qualitatively consistent with a power law, based on both the observed intensity distribution and the decrease of maximum observed intensity with the distance along Earth's surface between the sub-satellite point on the Earth and the TGF source position. We will write the power law form of the differential intensity distribution as $dn/dN = N^{-\lambda}$, where N is the number of counts detected by a given instrument. *Østgaard et al.* [2012] compared the observed brightness distributions of TGFs observed with the *Reuven Ramaty High Energy Solar Spectroscopic Imager (RHESSI)* and *Fermi* satellites, which have different sensitivities, to conclude that the power-law index λ was approximately 2.3 ± 0.2 over the sensitivity ranges of those two instruments. *Tierney et al.* [2013], using *Fermi* data alone, found a comparable value of 2.20 ± 0.13. *Marisaldi et al.* [2014], using the "normal" population of *AGILE* TGFs (those without individual counts >30 MeV), found a very similar index of $\lambda = 2.4$, noting that $\lambda = 2.2$ or 2.6 also gave similar results. These numbers refer to the distribution of observed intensities, which is a function of the true luminosity distribution at the source, the distribution in altitude, and the effects of distance and beaming.

In this paper we search not for individual TGFs but for the cumulative gamma-ray signal produced by a large number of lightning discharges (radio-bright intracloud discharges (IC) and cloud-to-ground discharges (CG)) beneath the *RHESSI* spacecraft. We identify the times and locations of these discharges using the World Wide Lightning Location Network (WWLLN) [*Lay et al.*, 2004; *Jacobson et al.*, 2006; *Rodger et al.*, 2008; *Hutchins et al.*, 2012a]. We then sum (stack) the gamma-ray "light curves" (histograms of count rate versus time), shifted in time so that $t = 0$ is the expected arrival time at *RHESSI* of a light-speed signal from the WWLLN event.

A statistically significant signal is detected, but it amounts to a very low average signal per flash (see §3.1). Since *RHESSI* has passed near millions of lightning discharges in the nine years of data we searched, the sensitivity to a weak average gamma-ray signal per discharge in the stacked sum is orders of magnitude better than the sensitivity to any individual TGF. Sensitivity in both the stacked analysis and the usual algorithms that search for *RHESSI* TGFs [*Grefenstette et al.*, 2009; *Gjesteland et al.*, 2012] is dominated by the Poisson variability in the background counts, which are mostly produced by cosmic ray interactions in the detectors, spacecraft, and Earth's atmosphere.

We have presented preliminary results from this method [*Smith et al.*, 2014], and *Østgaard et al.* [2015] used substantially the same method to get a similar primary result. *Østgaard et al.* [2015], however, emphasized the presence of the small revealed population of subluminous events that could be identified by searching the WWLLN flash times instead of searching *RHESSI* data at random. [*McTague et al.*, 2015] performed a similar search using radio data from the National Lightning Detection Network and gamma-ray data from the Gamma-ray Burst Monitor (GBM) on *Fermi*. They looked only at positive IC lightning events of high peak current (>15 kA), further selecting only those with specific VLF waveforms most closely resembling those associated with known TGFs, for a total of 1787 flashes. Like *Østgaard et al.* [2015], they also found a few faint but significant TGF candidate events; however, they noted that there were far fewer than expected given the power-law distribution of brighter TGFs, and their stacking analysis, like the one we present below, also showed a deficit of gamma-ray emission, such that no more than 1/40 of lightning flashes, even in their highly TGF-favorable selected subset of lightning, could produce a TGF yielding 1 or more photons in *Fermi* GBM.

Here, in keeping with our original approach [*Smith et al.*, 2014], rather than focusing on faint but individually significant events, we explore instead the implications of the very low *average* gamma-ray flux associated with WWLLN flashes, using a much larger but much more indiscriminate class of lightning than *McTague et al.* [2015].

This method is also an ideal way to address the possibility that there is a large population of TGFs – or another high-energy radiation mechanism – much shorter in duration than those currently known. The shortest values of t_{50}, the time interval containing containing the middle 50% of counts in a TGF, are about 30 μs in *Fermi* data [*Briggs et al.*, 2013] and 20 μs in *AGILE* [*Marisaldi et al.*, 2015]. But even just a few μs is a plausible time scale for a single step of a stepped leader or for a lightning initiation event stimulated by a large cosmic-ray shower in the atmosphere. Without the time-delays associated with Comptonization in the atmosphere, the orbiting observatories would have trouble distinguishing such an event from cosmic rays, some of which can produce showers in the spacecraft and cause several detectors to register counts. Thus at first blush such a population of TGFs could have been missed whether they are weak or strong. The stacking analysis presented below eliminates this confusion since even a single registered gamma-ray count, if it appears in a significant fraction of flashes, will add up to a strong signal in the stacked light curve, while cosmic ray events will occur no more often during lightning discharges than during other times.

But *Celestin and Pasko* [2012] showed that delays from Compton scattering lengthen an instantaneous release of TGF gamma-rays at 15 km into an event with t_{50} ranging from about 15 to 75μs as the radial distance to the subsatellite point goes from 0–500 km. Thus a population of super-short TGFs produced at ordinary TGF altitudes seems impossible to hide from the current generation of satellites. But a limit on very short gamma-ray emission is still worth setting to check the possibility of another high-energy radiation mechanism from lightning that might take place at high altitudes, and might be weaker than ordinary TGFs. In particular, high-altitude gamma-ray production appears in some early models of TGFs, published before the lower altitudes now generally accepted were even thought of, and connected with the production mechanisms of sprites [*Roussel-Dupré and Gurevich*, 1996; *Lehtinen et al.*, 1999] and elves *Inan and Lehtinen* [2005]. In these models, the spectrum produced is also that of RREA.

1.1. Observed versus intrinsic brightness distribution

Our analysis follows previous works in quantitatively discussing only the distribution of observed brightnesses at the spacecraft, rather than the intrinsic distribution of TGFs in total released energy [*Collier et al.*, 2011; *Østgaard et al.*, 2012; *Tierney et al.*, 2013; *Marisaldi et al.*, 2014; *McTague et al.*, 2015]. These are different for at least two reasons: the distribution of the TGFs in altitude, such that some suffer more atmospheric absorption than others, and the different radial distances from the subsatellite point for different TGFs. While the latter distribution should be entirely predictable (and uniform with surface area), the nature of the TGF beam (broad or narrow, tilted or vertical), must be determined from observations just as the altitude distribution is.

Carlson et al. [2012] quantified the connection between the intrinsic and observed distributions in the case where the latter is a power law, still assuming that all TGFs occur at the same altitude; the intrinsic distribution is found to be harder. *Nisi et al.* [2014] extended these calculations to include an altitude distribution of TGFs derived from tropopause data, showing that taking this into account softens the observed distribution even more relative to the intrinsic one. *Hazelton* [2009], taking both factors into account, used a model altitude distribution from tropical thunderstorm cloud top heights [*Ushio* *et al.*, 2001] as a proxy for TGF altitudes to estimate the fraction of TGFs that triggered *RHESSI*, and to find that an intrinsic intensity distribution with power law index −1.5 seemed consistent with the softer observed *RHESSI* intensity distribution.

Both *Østgaard et al.* [2012] and *Hansen et al.* [2013] suggest that all lightning could produce TGFs if they are faint enough not to be observed from space, and of course that is possible; and as far as space observations are concerned, it must also be possible that even bright TGFs could be associated with all lightning if most of them are hidden from observation from space by being either very low in the atmosphere or beamed downwards instead of upwards. As we discuss limits on the number of lightning flashes that can producing TGFs based on what is seen from orbit, we will have to consider two possibilities: that there is a very large population of very faint TGFs, and that there is a population of brighter TGFs (whether or not they are as bright as those seen from orbit) buried deep in the atmosphere. We will address the former possibility over the course of our analysis, showing that intrinsically faint TGFs produced in the same altitude range as the bright ones, if they exist at all, have to either make up a second low-luminosity peak in the TGF luminosity distribution, rather than being part of the same distribution as bright TGFs, or else be part of a rather finely-tuned monotonic distribution in which the average luminosity is so low that it resembles that of lightning stepped leaders rather than TGFs.

The other possibility – a population of deeply buried TGFs much larger than the population we see from space – we discuss here. We believe that the most recent available evidence suggests this is unlikely. When TGFs were thought to lie mostly in the range of 15–21 km [e.g. *Dwyer and Smith*, 2005], and the environment of their production was entirely a mystery, hiding a large population at much lower altitudes was very feasible. Now we are learning that TGFs are produced between the upper positive and main negative charge regions of storms, many at altitudes around 12 km [*Stanley et al.*, 2006; *Shao et al.*, 2010; *Lu et al.*, 2010; *Lu et al.*, 2011; *Dwyer and Cummer*, 2013; *Cummer et al.*, 2014, 2015; *Gjesteland et al.*, 2015] at mid latitudes, and presumably somewhat higher at equatorial latitudes where convective cells are taller on average. This has several implications.

Cummer et al. [2015] found in all three cases they studied that a TGF occurred when an upward negative leader reached a length of 1–2 km, in the middle of its journey from the main negative up to the upper positive region. *Lyu et al.* [2015] have identified what appears to be the characteristic radio signal of a TGF, or at least of a subset of TGFs, called a "positive energetic in-cloud pulse" (+EIP). Out of 27 +EIPs in North America, 23 lay between 10 km and 13 km, just the range of altitudes identified for TGFs in this geographic region [*Stanley et al.*, 2006; *Shao et al.*, 2010; *Lu et al.*, 2010; *Lu et al.*, 2011; *Dwyer and Cummer*, 2013; *Cummer et al.*, 2014, 2015]. Since the radio emission isn't subject to atmospheric attenuation as gamma-rays viewed from orbit are, to the extent that +EIPs and TGFs are the same population, this local and preliminary result suggests that there may be no deeply buried population of TGFs being missed from orbit. In addition, the number of reverse-polarity (negative) EIPs was much lower than the number of +EIPs, suggesting that there is no large hidden population of downward TGFs either, assuming their radio emission is similar.

Even if we ignore the evidence of the +EIP distribution until we are sure that +EIPs are really representative of TGFs, we can ask under what circumstances our results might still leave room for a much higher TGF/lightning ratio than we calculate. First, even going down as far as 8 km, below all the North American +EIPs and presumably even further below any tropical ones, there is only a factor of $\sim$ 40 decrease in the apparent intensity of a TGF from orbit relative to an origin at 12 km (using the atmospheric model of *Humphreys* [1964] and the e-folding depth of 45 g cm^{-2} for a TGF spectrum modeled by *Smith et al.* [2010]). Since at least one TGF observed by *RHESSI* was among the brightest it has seen despite originating at $\leq$12 km *Gjesteland et al.* [2015], it is possible that the brightest TGFs, at least, may be visible from orbit all the way down to the bottom of their production range. If the bright TGFs individually detected by *RHESSI* are just the high-altitude tip of an iceberg peaked at much lower altitudes, and there are many more TGFs down there, then qualitatively speaking there should be many weak TGFs seen from a few kilometers further down (e.g. within that factor of 40 or so of absorption). That would give exactly the sort of bright summed signal that we search for below and do not find.

That forces us to consider a more finely-tuned case in which there are still a lot of unseen TGFs at low altitude, but they tend to be intrinsically weaker than normal TGFs. TGFs both modest in intensity (but still bright enough to be considered of the same class of event) and biased toward relatively low altitudes may still be numerous; but we have no evidence of their existence, and a small amount of evidence against it from ADELE [*Smith et al.*, 2011].

Even ignoring the ADELE result, the scenario of many underluminous and low-altitude TGFs runs into a further difficulty. Lightning itself is much more common in storms that reach high altitudes than in those that don't, with the flash rate going approximately as the 4.9th power of the cloud top height [*Price and Rind*, 1992]. Thus the low storms that might harbor low-lying TGFs between their main negative and upper positive charge centers produce only a very, very small fraction of global lightning; and thus, TGFs produced in these storms cannot do a lot to boost the overall global TGF/lightning ratio, even in the highly tuned case where low-altitude storms produce TGFs at a much higher rate of efficiency but with much lower intrinsic luminosity. Figure 1 illustrates the effect of taking into account how much lightning storms at different heights produce. The solid curve is an approximation to the altitude distribution of thunderstorm cloud tops from *Ushio et al.* [2001], for the case of lightning over land in the tropics, the most relevant for most TGFs (see their Figure 5, where they show the cumulative distribution while we have fit their data to a smooth empirical curve and converted it to a differential distribution). Looking at this curve, you might expect that low-altitude storms could harbor a lot of missing TGFs. But the dashed curve multiplies this curve by the flash rate function of *Price and Rind* [1992], to give the distribution of storm heights measured *at the times of lightning flashes*. This is the more relevant curve for estimating TGF production altitudes (which should be a few km below the cloud top), and it is clear that it is more narrow in altitude than the curve that is uncorrected for flash rate.

2. Data Analysis Method

We included data from 2004 January 1 to 2012 December 31. All discharges localized by WWLLN were stored in a catalog if they occurred within 1200 km of the current sub-satellite point of *RHESSI*. The time-tagged gamma-ray counts in *RHESSI* near the time of each stored WWLLN discharge were captured from the raw *RHESSI* database using the SolarSoft package (http://www.lmsal.com/solarsoft/). The light-propagation time from the WWLLN discharge position was subtracted from the *RHESSI* event times, assuming a TGF altitude of 15 km, then the *RHESSI* clock correction of *Gjesteland et al.* [2014] was applied (+2.35 ms before 2005 August 5 and +1.82ms afterward). The time-tagged list of counts was then cleaned, a process that combines simultaneous interactions in multiple detectors into a single event (under the assumption of Compton scattering) and removes certain instrumental artifacts [*Smith et al.*, 2002]. The cleaned count lists corresponding to all WWLLN discharges were then combined into a single histogram, with time relative to the matching WWLLN discharge, in 1 ms bins being the x axis of the histogram. Summed histograms were made separately for *RHESSI*/WWLLN ground distances ranging from 0–100 km to 1100–1200 km so that comparisons could be made for both near and more distant lightning.

We further divided the histogram for each distance range into a histogram for the small fraction of WWLLN discharges that match closely (within 10 ms) with a known *RHESSI* TGF and the great majority that do not. In each case we looked for an excess in gamma-ray counts near $t = 0$; in the first case, of course, this signal should be very large, but in the second case it depends entirely on the unknown population of weak TGFs that cannot be recognized individually. Our primary results are the number of gamma-ray counts per WWLLN discharge in the unmatched sample and its ratio to the same excess in the matched sample.

The *RHESSI* catalog we used combines events from the first *RHESSI* catalog [*Grefenstette et al.*, 2009] and a new algorithm, still under development, that uses binning times from 60 μs to 3 ms to detect TGFs, as opposed to the single $\sim$ 1 ms binning of the first catalog. This combined catalog produces a total of 3277 TGFs from 2004–2012, with 477 matching WWLLN discharges within 10 ms and 1200 km. While the experimental algorithm contains a larger fraction of false positive detections than the first catalog, for this work we don't use the gamma-ray data from unmatched TGFs. Those TGF candidates that match a WWLLN discharge within 10 ms are vastly less likely than the rest of the sample to be false positive detections, since on average the probability of accidentally finding a WWLLN discharge within 1200 km of *RHESSI* within 10 ms is 3.4×10^{-4} (this rate is simply the total number of discharges during our 2004-2012 period within that distance divided by the duration of that period).

It is important to consider the effects of the imperfect sensitivity of both WWLLN and *RHESSI*. Early in this period, WWLLN was less sensitive than it was at the end. For some intervals within this period, *RHESSI* was less sensitive than usual due to radiation damage to its detectors, which are periodically annealed to reduce this effect [*Grefenstette et al.*, 2009].

In 2011, WWLLN was compared with the more sensitive Earth Networks Total Lightning Network (ENTLN) over the continental United States [*Hutchins et al.*, 2012b], and it was estimated that WWLLN's efficiency at that time was 4.2% for all discharges and 15% for CG strokes in particular. But for data taken at approximately the same time in the evolution of WWLLN's array, *Connaughton et al.* [2013] found WWLLN matches for 182 out of 601 *Fermi* TGFs, a 30% match rate. Most of these events took place in parts of the world where WWLLN's sensitivity is lower than in the continental United States as well, showing that WWLLN is much more sensitive to TGF-related lightning than to either non-TGF-related IC or CG lightning. We expect that relative sensitivity to hold even earlier in the evolution of WWLLN, when its overall sensitivity was lower. What this means for our analysis is that we are missing a much higher percentage of the lightning without TGFs than the lightning with TGFs; thus the values and upper limits for the gamma-ray counts per WWLLN discharge that we derive below are probably too high, and the constraints would become even stricter under a more detailed analysis incorporating WWLLN sensitivity as a function of time, position, and flash type. Note also that there are many bright TGFs that are not matched by WWLLN, particularly those of longer duration [*Connaughton et al.*, 2013], so that nothing in our work here should be construed as putting any limit on a potential population – even a very large one – of weak TGFs that are not connected to conventional lightning.

For the issue of *RHESSI*'s time-varying sensitivity, we note that when the detectors are damaged and counting fewer gamma-rays in each TGF, the fraction of counts lost will be comparable for the luminous TGFs that are detected and for the (presumed) subluminous TGFs that we are looking for from the unmatched WWLLN discharges. In that case the *RHESSI* sensitivity drops out to first order, since we express our results in terms of the ratio of gamma-ray counts from unmatched WWLLN discharges to those during WWLLN discharges matched to known TGFs.

We also consider the effect of *RHESSI*'s instrumental deadtime, which causes some counts to be lost during bright TGFs [*Grefenstette et al.*, 2009]. To the extent that this is an important effect, it would also result in even stricter upper limits on the sub-luminous TGFs than are quoted below, since the detected TGFs would suffer from deadtime much more than the faint, undetected ones. So the corrected ratio of gamma-ray counts in unmatched WWLLN discharges to matched ones would drop further if the latter were corrected for deadtime.

Finally, it is important to maintain the distinction between ruling out a TGF coincident with the specific discharge or return stroke seen by WWLLN and ruling out a TGF anywhere within the overall flash. *Omar et al.* [2014] found three types of association between TGFs detected by the *Fermi* Gamma-ray Burst Monitor (GBM) and lightning sferics recorded by the Earth Networks Total Lightning Network (ENTLN): those that are virtually simultaneous [e.g. *Connaughton et al.*, 2013], those in which the timing differs by a few milliseconds in either direction, and those in which the TGF precedes the radio signal by hundreds of milliseconds. Figure 2 shows the same pattern in our association of *RHESSI* TGFs and WWLLN sferics. In section 3 below, we set separate stacking limits for gamma-rays using different combinations of these three types of timing association with our database of WWLLN sferics.

3. Gamma-ray upper limits with distance, time offset, and energy

In this section we present and interpret gamma-ray upper limits on *RHESSI* counts associated with WWLLN discharges, as a function of three parameters: the distance (measured along Earth's surface) between the WWLLN location and the *RHESSI* subsatellite point, the time offset between the WWLLN time and the stretch of *RHESSI* data being searched, and the energy range of the *RHESSI* photons considered.

3.1. Limits over integrated distance ranges

To get preliminary upper limits that are both simple to understand and have good statistical significance, we wish to sum the gamma-ray data corresponding to all WWLLN discharges out to two radii: the radius at which the sensitivity of *RHESSI* to known TGFs begins to fall off, and the radius at which it has fallen nearly to zero. The former tells us primarily about subluminous TGFs in the distance range where we might expect that all typically bright TGFs would be seen, while the latter opens up the possibility of seeing events that might be typically bright, or nearly so, but appear fainter because of their distance.

Figure 3 shows the surface density of known TGFs as a function of the distance between the *RHESSI* subsatellite point and the WWLLN discharge position for all 477 known TGFs that occurred within 1200 km and 10 ms of a WWLLN discharge. This distribution is qualitatively similar to those reported by previous authors who used both *RHESSI* and *Fermi* TGFs [*Cummer et al.*, 2005; *Cohen et al.*, 2010; *Connaughton et al.*, 2010; *Collier et al.*, 2011; *Briggs et al.*, 2013]. The curve shown in the figure is a best-fit error function (integral of a Gaussian) with the 50% point at (403 ± 21) km and $\sigma = (174 \pm 20)$ km. This is purely a phenomenological function chosen to resemble the data. Figure 3 suggests that the TGF beam is either moderately broad ($\sim$ 400 km radius at $\sim$ 600 km altitude giving a half angle of 34°), or else, if narrower, distributed in tilt angle out to a comparable angle. The model of a somewhat broad beam is supported by spectroscopic results [*Hazelton et al.*, 2009; *Gjesteland et al.*, 2011]. Below, we use 0–300 km to represent the range where we have nearly constant sensitivity to known TGFs, and 0–700 km for a range that could include a significant number of TGFs that are typically bright intrinsically, but not identified because they are distant.

Figures 4 and 5 show, in their top panels, the stacked gamma-ray histograms for the WWLLN discharges that were matched to a known *RHESSI* TGF within 10 ms (top panel) and those that were not matched to any *RHESSI* TGF within 1 s (bottom panel). Figure 4 runs out to 300 km and includes 216 known TGFs in the top panel and 432,342

WWLLN flashes in the bottom panel; Figure 5 runs out to 700 km and includes 461 known TGFs in the top panel and 2,338,292 WWLLN flashes in the bottom panel.

The expectation is that a population of under-luminous TGFs would make a significant signal when summed together. The TGF-matched discharges show a dramatic peak, as expected. To calculate the average number of counts in a TGF, we sum the central four milliseconds of the figure and subtract the average background, averaged from 0.1 to 1 s in the direction of the WWLLN sferic leading the TGF. This range is chosen with reference to Figure 2, since it appears that there are not a significant number of known TGFs in this range of time offset. Table 1 shows the number of gamma-ray counts per WWLLN flash, its error bar, statistical significance, and upper limit at 95% confidence for the two distance ranges and for both the known TGFs and the WWLLN discharges without a known TGF. For the known TGFs, the error is the 1σ statistical error on the average; of course the variance in the number of counts in each TGF is much higher [*Grefenstette et al.*, 2009].

Table 1 includes gamma-ray count limits for five time ranges relative to the WWLLN flash in which known TGFs appeared in Figure 2 and in the work presented by *Omar et al.* [2014]: within 2 ms (essentially simultaneous, but allowing for inclusion of most of the flux of the longest-duration TGFs – "group I" in Figure 2); between 2 ms and 10 ms in either direction (group II); within 10 ms in either direction (group I plus group II, intended to encompass all processes in the upward-going leader, regardless of which one triggers WWLLN); between 200 ms and 800 ms in the sense of the TGF preceding the WWLLN detection (group III); and the sum of all three time groups, intended to account for any likely time the gammas might appear relative to WWLLN. Most known TGF/WWLLN matches are simultaneous (Figure 2), but it is reasonable to suppose that if a TGF can be under-luminous, the sferic pulse associated with the TGF current would become less likely to be the one to trigger WWLLN. Then, if there is a TGF at all, it would be more likely to fall into one of the other two groups of *RHESSI*-WWLLN time difference.

The total detected signals for WWLLN discharges without a known TGF are small, and that from 0–300 km does not constitute a significant detection. As shown in the third line of Table 1, the upper limit at 95% confidence is (1.24×10^{-2}) *RHESSI* counts per WWLLN flash, or 7.82×10^{-4} times the intensity of an average *RHESSI* TGF. As we mentioned in section 2 above, *RHESSI's* deadtime during the known TGFs and WWLLN's preferential sensitivity to TGF-producing lightning both produce biases that, if corrected, would result in making these limits even stricter.

Assuming that not all discharges produce a TGF, even a subluminous one, the upper limits can be re-interpreted as a function of the fraction of discharges considered to be candidate TGF producers. The solid lines in Figure 6 illustrate this; all points along each line give the same value, that tabulated in the last column of Table 1, for the upper limits on TGF intensity per WWLLN flash from 0–300 km (relative to an average TGF of 15.85 counts). The curves are shown under three assumptions: that the TGF is simultaneous with the WWLLN signal (group I, as studied by *Østgaard et al.* [2015]), that the TGF and WWLLN signal are both somewhere in the upward progression of the initial leader (group I + group II) and that the TGF/sferic relation could be in any of the three groups identified in Figure 2. For the first two timing assumptions, these curves show that TGFs with anything even approaching the intensity of the known population are relatively rare;

Table 1. *RHESSI* counts per WWLLN flash, measured values and limits, versus distance range and relative timing

Case	Range	dT[a]	Counts/flash	Error (σ)	Value/error	95% limit	95% frac. limit[b]
TGF	0–300 km	1	15.85	0.32	50	16.38	1.033
TGF	0–700 km	1	14.89	0.22	69	15.25	1.024
No TGF	0–300 km	1	6.23×10^{-3}	3.76×10^{-3}	1.66	1.24×10^{-2}	7.82×10^{-4}
No TGF	0–700 km	1	7.43×10^{-3}	1.62×10^{-3}	4.60	1.01×10^{-2}	6.78×10^{-4}
No TGF	0–300 km	2	-6.85×10^{-4}	7.57×10^{-3}	-0.09	1.18×10^{-2}	7.44×10^{-4}
No TGF	0–700 km	2	1.96×10^{-3}	3.25×10^{-3}	0.60	7.31×10^{-3}	4.91×10^{-4}
No TGF	0–300 km	3	6.54×10^{-2}	5.93×10^{-2}	1.10	1.63×10^{-1}	1.03×10^{-2}
No TGF	0–700 km	3	-5.47×10^{-3}	2.55×10^{-2}	-0.21	3.65×10^{-2}	2.45×10^{-3}
No TGF	0–300 km	1+2	5.54×10^{-3}	8.48×10^{-3}	0.65	1.95×10^{-2}	1.23×10^{-3}
No TGF	0–700 km	1+2	9.39×10^{-3}	3.65×10^{-3}	2.58	1.54×10^{-2}	1.03×10^{-3}
No TGF	0–300 km	1+2+3	7.08×10^{-2}	6.07×10^{-2}	1.17	1.71×10^{-1}	1.08×10^{-2}
No TGF	0–700 km	1+2+3	3.83×10^{-3}	2.61×10^{-2}	0.15	4.67×10^{-2}	3.14×10^{-3}

[a] Time difference range code, *RHESSI*–WWLLN. 1: -2 to +2 ms, group I; 2: -10 to -2 and +2 to +10 ms, group II; 3: -200 to -800 ms, group III.

[b] 95% confidence upper limit expressed as a fraction of the average counts from known TGFs for that distance range and simultaneous timing.

under the third assumption, in which 620 ms of background has to be included when calculating the limits, the constraint is not as severe.

One physically-motivated reason to focus attention on only a subset of lightning is the lack, to date, of any reported TGF observed from space in conjunction with cloud-to-ground lightning. This may be due to the TGF mechanism requiring the fields generated when a new leader of one sign (e.g. an upward-moving negative leader) approaches a charge region of the opposite sign (e.g. the upper positive charge center in a simple tripolar thunderstorm). So we attempt, in the simplest possible way, to estimate the limit on gamma-ray counts per WWLLN-detected +IC flash, instead of per any WWLLN flash. WWLLN doesn't report flash type, but a comparison with NLDN data over the continental United States [*Abarca et al.*, 2010] from 2006–2009 gave an average ratio of 2.15 for the WWLLN detection efficiency of CG to IC lightning. This ratio was relatively constant from 2006 to 2009, a period in which the absolute efficiency of WWLLN was increasing rapidly, so for this simple calculation we feel justified in using it for the entire *RHESSI* database, for which the 2006–2009 period represents the central third. Assuming a conservative IC/CG ratio of ~ 3 averaged over *RHESSI's* view of the tropical and temperate globe (see, e.g., Figure 1 of *Boccippio et al.* [2001]), we expect that roughly 58% of the WWLLN sample is IC lightning (*Østgaard et al.* [2015] used the same references and reached the same conclusion). Due to the limitations of WWLLN's sensitivity, most of the +IC lightning in the sample is going to be that which contains either a narrow bipolar event (NBE) or a +EIP, the latter perhaps the direct current signal of TGFs themselves [*Lyu et al.*, 2015]. If we consider most of this IC lightning to be positive lightning due to upward negative leaders, which might be expected to be capable of producing a TGF, our WWLLN upper limits are increased (weakened) by a factor of 1/0.58 = 1.7. We emphasize that this is not a correction to our results in Table 1, it's the answer to a different question: what is the gamma-ray yield of +IC lightning, as opposed to the gamma-ray yield of WWLLN-detected lightning in general? The dashed lines in Figure 6 differ from the solid ones in including this factor.

As promised in the Introduction, we can interpret the limits of Figure 6 as limits not only on weak but otherwise conventional TGFs, but also on RREA of much smaller duration, which would be mistaken for cosmic ray showers in the spacecraft by the TGF-detection algorithm. Because of Comptonization broadening [*Celestin et al.*, 2012], these short events (say 10μs or shorter) must occur at high altitudes, due to some exotic mechanism. This interpretation doesn't affect the values of the limits on counts per flash, but it does suggest which of the values presented in Figure 6 might be most relevant. For example, considering the electromagnetic pulse (EMP) mechanism [*Inan and Lehtinen*, 2005] leads us to look primarily at the "group I only" timescale, since presumably the brightest EMP during a flash is both most likely to produce gamma-rays and most likely to trigger WWLLN. The current analysis is not well suited for searching for sprite-related gamma-rays, however, since these are expected to occur with a large delay between the sferic (usually +CG) and the high-altitude breakdown presumably producing gamma-rays. This is a time window we do not examine (the opposite sense of delay to group III), although we can see from Figure 2 that there are not a statistically significant number of detections of normal TGFs in this window. In addition, since only a very small fraction of lightning produces sprites, only a search targeting sprites, or at least lightning with a very large charge moment change suggesting it might have made a sprite, will be usefully sensitive.

3.2. Limits versus narrow distance band and energy

Figures 7 and 8 show the basic result of the analysis (counts/WWLLN flash) as a function of ground distance, using rings 100 km wide instead of the ranges 0–300 km and 0–700 km discussed above. In Figure 7 we show the results separately for the three relative time ranges derived from Figure 2 (groups I, II, and III). In Figure 8 we explore three energy ranges: the whole detectable range for *RHESSI*'s rear detector segments (roughly 30 keV to 17 MeV), which was used for all the results above, and also the two bands above and below 500 keV. Above this energy, the spectrum has a significant component of non-Comptonized gammas, and below it is dominated by multiply-Comptonized gammas [*Dwyer and Smith*, 2005]. In both Figures, the black data points with error bars represent the measurement for the WWLLN flashes with no known TGF, and the red data points add in the few WWLLN flashes associated with known TGFs as well.

The top panel of Figure 7 shows that at small radii, the entire population of WWLLN flashes without a TGF contributes about the same number of gamma-rays to the sum as the known TGFs. Since there are 2,000 times as many WWLLN flashes without known TGFs as with, this is another way of expressing the paucity of gamma radiation outside the known TGFs. Breaking down the results by distance shows something else important: the most significant excess is in the 400–700 km range. This suggests that most of the excess, which, as shown above, is already quite small, is due not to truly subluminous TGFs but rather to normally bright TGFs that are faint at the spacecraft only because of their distance and beaming. This is implicit in the differences shown in Table 1 for the

0–300 km range (no significant detection) and the 0–700 km range (significant detection), but is made clearer by Figure 7. The importance of the $>$ 400 km distance range to finding new TGFs was also noticed by *Østgaard et al.* [2015], who found that 50% of their newly discovered, subluminous events were found in the 400–800 km range. We note that in the population of 477 bright, normally detected TGFs with WWLLN counterparts (Figure 3), only 135 (28.3%) were found at $>$ 400 km.

The following two panels of Figure 7 show that there is no distance band in which there is a statistically significant gamma-ray signal for either of the non-simultaneous *RHESSI*/WWLLN time difference groups.

The top panel of Figure 7 also shows two theoretical distributions, based on simulations of a relativistic runaway avalanche propagated through models of Earth's atmosphere and the *RHESSI* spacecraft [*Dwyer and Smith*, 2005; *Hazelton et al.*, 2009]. The simulated source altitude is 13 km, but the shape of the curves is not very sensitive to altitude. The blue curve ("Narrow") represents the natural minimum angular source width due to electron scattering and bremsstrahlung production (about 18° full width at half maximum when the photons are first created – see Figure 2 of *Hazelton et al.* [2009]), while the green curve ("Broad") has all the photons at the time of their creation redistributed into a distribution isotropic within, but confined to, a half opening angle of 45°. These curves, which are shown with an arbitrary normalization, should be compared in shape to the red diamonds, which represent the sum of gamma-rays from all WWLLN flashes, whether they correspond to a known TGF or not.

Since even the result of the broad TGF model is not as broad as the true distribution, we can conclude that the signal at small radial distances from the brighter (e.g. known)

TGFs is badly suppressed by instrumental deadtime. This conclusion is supported by the observation [*Grefenstette et al.*, 2009] that in nearly all known *RHESSI* TGFs the instrument is counting at its maximum throughput at the peak of the event, as well as by the recent discovery of a class of *RHESSI* TGFs, roughly 3% of the total, that completely paralyze the instrument at their peaks and are detected primarily by the delayed, Comptonized tail [*Kelley et al.*, 2015]. This suggests that the average number of counts in the known TGFs is too low, probably by a factor of 2 or more, which would make the limits in the last column of Table 1 and in Figure 6 lower (more restrictive) by the same factor, assuming that the unidentified, faint TGFs are not themselves affected by deadtime. We note that *Østgaard et al.* [2012] estimated an average *RHESSI* TGF deadtime of only 26%, but they appear to have made the conservative assumption that every TGF was on the rising part of curve of registered counts vs. true counts [*Grefenstette et al.*, 2009]. The new results on *RHESSI* TGFs that reach 100% deadtime at their peak suggest that many other TGFs, although they fall short of paralysis at their peaks, likely also have >50% deadtime, so that assumption needs to be revisited.

Figure 8 shows only the data for the near-simultaneous relative time range. The top panel is the same data as the top panel of Figure 7. In the following panels, the counts above and below 500 keV are shown separately. While no data point is highly significant except the 600–700 km band at low energies, the overall trend is for the low-energy photons to reside at larger distances than the high-energy ones. This is consistent with the expectation that distant events are dominated by either the Compton tail alone or else the intrinsically softer spectrum at the edge of the bremsstrahlung beam [*Østgaard et al.*, 2008; *Hazelton et al.*, 2009].

3.3. Constraining broken power-law distributions

Table 1 gives our limits on the average gamma-ray intensity of a typical WWLLN flash relative to a typical known *RHESSI* TGF. Here we use the same limits to constrain the distribution of TGF intensities under the assumption that it has the form of a power law on the bright end [*Collier et al.*, 2011; *Østgaard et al.*, 2012; *Tierney et al.*, 2013; *Marisaldi et al.*, 2014] breaking to a flatter index or cutting off completely below a threshold, the threshold being at or below *RHESSI*'s individual detection level.

We define the differential intensity distribution of TGFs, dn/dN, over the range where TGFs are detectable by *RHESSI*, as a power law $N^{-\lambda}$, with $\lambda = 2.3$ being the expected value [*Østgaard et al.*, 2012; *Tierney et al.*, 2013; *Marisaldi et al.*, 2014] and N in units of *RHESSI* counts. We do not attempt to derive the number of relativistic electrons or gamma-rays at the source, which requires knowledge of the altitude distribution and the beam opening angle. This is consistent with the approach of the other authors. An index of $\lambda = 2.3$ must flatten or turn over at low intensities to prevent the total number of TGFs from becoming infinite – and must do so even sooner to prevent it from exceeding the number of potentially TGF-producing lightning discharges. But since there are far more lightning discharges than detected TGFs, this break could in principle be orders of magnitude below the lower sensitivity limit of *RHESSI*. Instead, with the strong limits from our stacked analysis, we can now show that the break is, in fact, quite close to the instrumental sensitivity limit. Of course, the broken power law could be replaced with a distribution that flattens more continuously toward low intensity, but we cannot evaluate all possible distributions, and no particular functional form has been theoretically predicted.

There have been hints of flattening being observed close to the lower intensity limits already. *Marisaldi et al.* [2014] noted that a flattening at lower count rates improved their $\lambda = 2.4$ fit to *AGILE* data, although they thought that might be attributable to their selection criteria. *Østgaard et al.* [2015], looking at *RHESSI*/WWLLN matches without previously identified TGFs, found a small population of new, individual, faint TGFs with a power-law index of 1.85. *McTague et al.* [2015] found a highly significant deficit of *Fermi* GBM TGFs with 6–9 counts relative to those with a higher number of counts that could be identified without a coincidence with known lightning.

We first examine the case where the index above the break is fixed at $\lambda = 2.3$. The normalization of the distribution above the effective *RHESSI* detection threshold (~ 13.625 counts; see Appendix) is determined by the fraction of WWLLN discharges with detected TGFs. A variety of indices λ_0 below the break are tested, and, for each, the 95% upper limit from the stacked gamma-ray observation (Table 1, penultimate column) is used to set a value for the position of the break in *RHESSI* counts. At this point, the distribution function for a given λ_0 is completely constrained, and can be integrated to give the fraction of WWLLN discharges that produce any TGF, including those in the part of the distribution that cannot be detected individually by *RHESSI*. The details of the calculation are given in the Appendix, and the results are shown in Table 2 and Figure 9 for the 95% upper limits on TGFs simultaneous with WWLLN (group I) and at any point within 10 ms (groups I + II).

All the models must break within an order of magnitude, and sometimes within a factor of 2, of the effective *RHESSI* threshold. As was also the case for the results of the previous section (Figure 6), considering only +IC flashes as candidates for TGF production would loosen the constraints (lower the break points), while accounting for deadtime, if it were accurately knowable, would tighten them. In Table 2 we show the total percentage of WWLLN flashes that produce a TGF of any brightness given each of the models in Figure 9. Recall that these are 95% upper limits on what the data will allow; the most likely values are therefore even lower, and the number of counts at the break even higher.

Values of $\lambda_0 \geq 1$ give an infinite number of TGFs, which of course is not physically possible, nor is a number of WWLLN-associated TGFs exceeding 100% of the lightning flashes in the WWLLN sample (we consider multi-peaked TGFs to be a single TGF; in most cases of double-peaked TGFs, both peaks would be contained in the 4 ms wide "group I" bin, and virtually all known multi-peak TGFs would be summed into the 20 ms wide "group II" bin). As λ_0 asymptotically approaches 1 from below, the percentage of flashes with a TGF grows larger, and the average counts per TGF smaller. It is not inevitable that these solutions are allowed; tightening the limit for group I (top panel of Figure 9) by just a factor two would make all solutions with $\lambda_0 \geq 0.6$ invalid by pushing the break point up into the regime where TGFs have been measured and found to have the 2.3 index. Such a tightening would probably be found to be the case if we could accurately understand *RHESSI*'s deadtime during the bright, known TGFs. But there is some room for flexibility on this constraint for two reasons: first, none of the published analyses are sufficiently powerful to reject at least a little hardening at the bottom of the range of individually detected TGFs, and, second, the detection threshold of *RHESSI* is not sharp, due to variations in background and detector efficiency with time (see Figure 12 in the Appendix).

To facilitate comparison with the results of *Østgaard et al.* [2012] combining *RHESSI* and *Fermi* data and the ADELE detection and upper limits, we examing one more specific model: one that breaks from 2.3 to 1.7 just at our calculated average *RHESSI* detection threshold of 13.625 counts (see Appendix), and then cuts off abruptly at a lower value, which is adjusted to match the 95% upper limit from the 0–300 km stacking analysis, as the power-law break position is adjusted in the other cases. The results of this model – the cutoff position and total percent of TGFs – are shown as the last row in Table 2 and the dotted line in Figure 9. *Østgaard et al.* [2012] didn't specify a particular point for the break to index 1.7; in their text they suggest it might be as low as 1/3 the *RHESSI* threshold, but their Figure 4 shows it at perhaps 35 observed *RHESSI* counts, or well above the threshold. As a compromise, we place the break at the threshold (as we define it), which is close to the middle of these possibilities and happens to make the calculations more convenient as well (see Appendix). We find, for this model and for our group I (simultaneous) time interval, 0.29% of lightning being allowed to contain a TGF anywhere in the distribution, considerably lower than the 2% estimated by *Østgaard et al.* [2012] when using only the ADELE nondetections to set limits on the weaker events.

It is always possible to define a function that will give a 100% yield of TGFs, as long as the definition of a "TGF" can be something that is very faint indeed as seen from orbit. In this work, with the exception of the dotted line case in Figure 9, we survey only power laws with a single break. For the cases where λ_0 approaches 1 from below and the percent of flashes producing a TGF starts to increase beyond 1%, it is important to examine what most of these TGFs would look like. For example, in the red curve in the bottom panel of Figure 9, $\lambda_0 = 0.99$ and 18.84% of WWLLN flashes are expected to produce a TGF. But

90% of these "TGFs" would be below the level of 3.5×10^{-4} *RHESSI* counts, or 2.6×10^{-5} of a threshold *RHESSI* TGF; and the average event within this 90% has 3.5×10^{-6} *RHESSI* counts, or 2.6×10^{-7} the intensity of a threshold TGF, if produced at the same altitude. We would contend that in that case, labeling most of the events allowed at low intensity as "TGFs" would be a misnomer. In fact, this is far from hypothetical. Since negative leaders seen near the ground often produce their own high-energy emission, with a softer spectrum and a luminosity on the order of 10^{-6} of a TGF [e.g. *Saleh et al.*, 2009], it is likely that all upward negative leaders in +IC lightning produce high-energy radiation at some level. In Table 2, in addition to the total percentage of lightning giving TGFs in each of the distributions, we also show the percentage of lightning giving TGFs with greater than 10^{-4} the brightness of a *RHESSI* threshold TGF, or $> 1.36\times10^{-3}$ *RHESSI* counts (see Appendix A). We select this value somewhat arbitrarily as the point where the luminosity is significantly more than that of a stepped leader and we would consider it to fall more in the category of a very weak TGF.

This argument extends even more clearly to other intensity distributions that would be allowed by our constraints. We can imagine a function that looks like the blue curves in Figure 9 ($\lambda_0 = 0$), with a second break back upwards to a steeply falling spectrum at a much lower count level, and then a sharp cutoff below that point such that the curve integrates to 100%. A function like that would be allowed by virtually any limit we can produce using this method, but it would embody two populations – a set of bright TGFs already known and a very different population at low luminosity. An extreme example of this is implicit in Figure 6, where 100% of WWLLN lightning flashes seem to be allowed to have a TGF within ±10 ms of brightness 0.001 of an average TGF; however, this can only be accommodated if the known power law distribution of normal TGFs cuts off completely and immediately below the *RHESSI* threshold – something that is not only quite artificial but also contradicted by the better sensitivity of *Fermi*, which finds real TGFs a bit below *RHESSI*'s threshold [*Østgaard et al.*, 2012].

We emphasize that we are not offering evidence for a low-luminosity component in any way; we are merely pointing out that the models we have explored with λ_0 approaching 1, and also more complicated models that we haven't explored, would allow such a component. But if this component were allowed to approach a significant fraction of lightning flashes, then either these "TGFs" would have to be part of a very different brightness distribution than the normal ones – perhaps peaked at low brightness – or if they were part of a continuous distribution, as we saw in the case of $\lambda_0 = 0.99$ for our particular family of models, the shape of that distribution would have to be rather finely tuned and the average brightness of a "TGF" would still be so low that we would argue they should not be classed as the same phenomenon. As noted above, we define a "TGF" as being both at least 10^{-4} of the brightness of a TGF near *RHESSI*'s threshold, and belonging to a monotonic or single-peaked distribution of brightnesses that includes the observed *RHESSI* TGFs. Within this definition, and with other caveats discussed in §1.1, the results of this section show that TGFs are rare; and we stress that for most of the distributions modeled, the TGF percentage of WWLLN lightning is less than 1% even if the brightness threshold is not imposed.

Leaving aside the distributions that contain many events so faint that they are more like stepped-leader emissions than TGFs, the range of breaks explored in Figure 9 suggests some additional generality. Since the result that > 99% of WWLLN flashes do not contain a TGF – not even one below *RHESSI*'s detection threshold – is robust for a wide range of shapes below *RHESSI*'s threshold, any hypothetical distribution that joins the $\lambda = 2.3$ curve above the detection threshold and flattens out to something flatter than $\lambda_0 = 0.5$, even if the transition is smooth rather than abrupt, is likely to give the same result. And, as Figure 9 shows, this conclusion holds whether you consider a potential TGF as occurring simultaneous with the WWLLN event or anywhere within 10 ms of it.

Although $\lambda = 2.3$ now has considerable support in the literature, we explore other values for completeness. Figures 10 and 11 show the break value in counts and total intensity-integrated percentage of TGF production for a range of combinations of λ and λ_0. The models for $\lambda = 2$ are evaluated at $\lambda = 2.001$ in order to escape division by zero (see equation A5). Cases where the break has to be pushed above the mean detection threshold of 13.625 counts have been left blank (white) in Figure 10. The TGF percentages of WWLLN lightning (bottom panels in Figures 10 and 11) are shown both with and without the cutoff at 10^{-4} of a *RHESSI* threshold TGF.

4. Discussion

Returning to the timing association between known TGFs and WWLLN sferics (Figure 2), we note that *Omar et al.* [2014] pointed out that this pattern is consistent with the picture of TGFs being generated in middle of the original upward progression of the negative leader in a positive IC flash. The strongest signal during this propagation, which is what the sferic networks will fix on, may be the TGF current itself [*Dwyer and Cummer*, 2013; *Cummer et al.*, 2014, 2015; *Lyu et al.*, 2015], yielding a simultaneous detection, or another event such as an NBE during the upward progression [*Stanley et al.*, 2006; *Shao et al.*, 2010], giving an offset of a few milliseconds in either direction. The events in which the sferic networks trigger from roughly 200 to 800 ms after the TGF would involve cases where the dominant sferic caught by the networks was associated with a subsequent process within the IC flash (e.g. the currents responsible for K changes, in which horizontal breakdowns occur that couple new regions of charge into the established channel). It is interesting that there seem to be no TGFs generated during these processes; if there were, we would expect a significant number of events in which the recorded sferic occurs during the leader ascent and the TGF several hundred milliseconds later. This is consistent with the observed absence of TGFs in CG lightning, which can also include similar horizontal breakdowns after the initial leader and first return stroke.

Østgaard et al. [2015] demonstrated how starting from radio signals allows a deeper search for individual gamma-ray excesses than can be accomplished by blindly searching the gamma-ray data, and they emphasized the new population of low-count TGFs that can be identified in this way. This population contributes to the excess that both they and we measure when summing *RHESSI* gamma-ray data at the times of WWLLN flashes. Because we use a different radio-blind triggering algorithm for the brighter TGFs, and because we use different years, different time binning, and different radial bands, our results can't be expected to be identical. For the case of simultaneous comparison, using the radial range 0–800 km, they found 3.92×10^{-3} counts per WWLLN flash (2903 excess counts in 740,210 flashes), a bit less than a factor of 2 below our value of 7.43×10^{-3} from row 4 of Table 1. Note that the difference would be in the direction of deriving even stronger constraints on faint TGFs if applying our analysis methods to their measurement. There is no contradiction here. Starting from roughly similar stacked *RHESSI* results, we have simply chosen to address different sides of the question: how new TGFs can be identified in the case of *Østgaard et al.* [2015], versus what is the limit on how many faint ones there could be in our case. For that purpose, it was necessary that we take a wider time bin for group I (4 ms instead of the 300 μs used by *Østgaard et al.* [2015]), because our goal was not the highest possible signal-to-noise ratio, as in their search, but rather to be certain that no flux was being unfairly discarded. Our conclusion is similar to that of *McTague et al.* [2015] from *Fermi*/GBM and NLDN data: that there is a strong turnover in the TGF intensity distribution on orbit not far below the detection threshold of the current missions in space.

The upcoming *Atmosphere-Space Interactions Monitor (ASIM)* on the International Space Station will be well positioned to look for this turnover, given its large effective area and factor of 2 advantage is sensitivity due to an orbital altitude lower than that of the spacecraft studying TGFs to date. Further observations within the atmosphere, from aircraft and balloons, and in a wider variety of meteorological environments than ADELE sampled, would provide critical proof of the arguments against a low-altitude population of TGFs given in §1.1.

Further modeling of the connection between observed and intrinsic brightness distributions should concentrate on model altitude distributions informed by lightning population data (e.g. Figure 1) and VLF studies of TGFs, in the context of intrinsic brightness distributions more complex than the simple power laws considered by *Hazelton* [2009] and *Nisi et al.* [2014].

Eventually, models of TGF generation should explain the observed luminosity distributions. *Celestin et al.* [2015] present a theoretical framework that unifies the stepped-leader x-ray emissions in CG lightning with TGFs, modeling both as cold runaway in a leader tip. They suggest the possibility of a population of subluminous TGFs that can't be individually detected by satellites, originating in leaders with a potential drop somewhat lower than the 300 MV they describe as being necessary to produce a TGF. While this seems to contradict the upper limits we present, we don't believe this is necessarily the case; they also find that the gamma-ray yield drops very quickly with the leader potential drop, so that a relatively flat distribution of potential drops could produce only a small number of TGFs of less than normal, but still substantial, brightness, which could perhaps still be allowed by our constraints.

Acknowledgments.

The authors wish to thank the World Wide Lightning Location Network (http://wwlln.net), a collaboration among over 50 universities and institutions, for providing the lightning location data used in this paper. *RHESSI* TGF data are available on an interactive and customizable website at `http://scipp.pbsci.ucsc.edu/rhessi/`. The specific WWLLN and *RHESSI* data tables used to produce the figures in this paper, and the analysis software, can be obtained by contacting the first author.

D.M.S. thanks Gerd Infanger for noting an error in our statistical methods. We thank the referees for useful comments that enabled us to strengthen both our quantiative analysis and qualitative arguments. This work was supported by award AMT-0846609 from the National Science Foundation.

Appendix A: Constraining the Broken Power Law

The results in Figures 9 through 11 are derived as follows. We define these symbols:

M is the number of WWLLN discharges without a known TGF, e.g. 432,342 for 0–300 km radial offset

T is the number of WWLLN discharges with a known TGF, e.g. 216 for 0–300 km

$f_{\rm obs} = \frac{T}{M+T}$ is the fraction of WWLLN discharges that make a known TGF, e.g. 5.0×10^{-4} for 0–300 km

f is the fraction of WWLLN discharges that make any TGF, known or not

N is the number of counts per TGF

$\frac{dn}{dN}$ is the distribution of the number of TGFs per flash as a function of number of counts in the TGF.

N_0 is the number of counts at the power-law index break

N_1 is the number of counts below which a single TGF will not be seen by *RHESSI*

λ is the power law index above the break, positive for a falling distribution

λ_0 is the power law index below the break

C is the number of counts per discharge over the M discharges with no known TGF

We take theoretical models of $\frac{dn}{dN}$ in the form of a broken power law matched at the break,

$$\frac{dn}{dN} = \begin{cases} AN_0^{\lambda_0-\lambda}N^{-\lambda_0} & N < N_0 \\ AN^{-\lambda} & N > N_0 \end{cases} \tag{A1}$$

Now we get the normalization constant A under the assumption that this should integrate to f. To avoid an infinite value for the integral, we require $\lambda_0 < 1$; while $\lambda > 2$ is also required to avoid an infinity in the total number of photons in all TGFs, we are able to examine cases with $\lambda < 2$ by assuming a cutoff at very high intensities; the analysis is insensitive to such a cutoff. In practice there must be such a cutoff for any λ, due to the finite amount of energy available in the thunderstorm creating any single TGF.

$$A = N_0^{\lambda-1} \frac{(1-\lambda_0)(1-\lambda)}{\lambda_0 - \lambda} f \tag{A2}$$

Integrating just over the range of detectable TGFs, we find

$$f_{\rm obs} = \int_{N_1}^{\infty} A N^{-\lambda} dN = \frac{A}{\lambda - 1} N_1^{1-\lambda} = \frac{\lambda_0 - 1}{\lambda_0 - \lambda} \left(\frac{N_1}{N_0}\right)^{1-\lambda} f \tag{A3}$$

or

$$f = \frac{\lambda_0 - \lambda}{\lambda_0 - 1} \left(\frac{N_1}{N_0}\right)^{\lambda-1} f_{\rm obs} \tag{A4}$$

The measured value (or upper limit) for counts/discharge excluding known TGFs becomes:

$$\begin{aligned} C &= \int_0^{N_0} A N_0^{\lambda_0-\lambda} N^{1-\lambda_0} dN + \int_{N_0}^{N_1} A N^{1-\lambda} dN = \frac{A}{2-\lambda_0} N_0^{2-\lambda} + \frac{A}{2-\lambda}(N_1^{2-\lambda} - N_0^{2-\lambda}) \\ &= N_0 \frac{(1-\lambda_0)(1-\lambda)}{\lambda_0 - \lambda} \left(\frac{1}{2-\lambda_0} + \frac{1}{\lambda - 2}\left[1 - \left(\frac{N_1}{N_0}\right)^{2-\lambda}\right]\right) f \end{aligned} \tag{A5}$$

For a chosen λ and λ_0 (neither is constrained by the stacking analysis) equations A4 and A5 together can be solved numerically to find the unknown break N_0 and the total fraction of discharges containing a TGF belonging to the distribution, f.

We also present a model, after *Østgaard et al.* [2012], where the index $\lambda = 2.3$ breaks to a harder index (they estimated $\lambda_0 = 1.7$) just at the detectability threshold of *RHESSI* (N_1) before cutting off abruptly at a lower number of counts, which we call N_2, determined by the 95% upper limits given in Table 1. In this scenario,

$$\frac{dn}{dN} = \begin{cases} 0 & N < N_2 \\ A N_1^{\lambda_0-\lambda} N^{-\lambda_0} & N_2 < N < N_1 \\ A N^{-\lambda} & N > N_1 \end{cases} \tag{A6}$$

$$A = f \left[\frac{N_1^{1-\lambda}}{1-\lambda_0} \left(\frac{\lambda_0 - \lambda}{1-\lambda} - \left(\frac{N_2}{N_1}\right)^{1-\lambda} \right) \right]^{-1} \tag{A7}$$

$$f = \frac{1}{1-\lambda_0}\left[(\lambda-\lambda_0) + (1-\lambda)\left(\frac{N_2}{N_1}\right)^{1-\lambda_0}\right] f_{\mathrm{obs}} \tag{A8}$$

$$C = \frac{A N_1^{\lambda_0-\lambda}}{2-\lambda_0}\left(N_1^{2-\lambda_0} - N_2^{2-\lambda_0}\right) \tag{A9}$$

For both types of model above, although we have chosen a single value for detectability threshold N_1, it varies with time for a number of reasons, including variation of gamma-ray background as a function of the orbital position of *RHESSI* and the changes in *RHESSI*'s efficiency for detecting TGF gammas due to radiation damage of its detectors [*Grefenstette et al.*, 2009]. In that paper, we chose a hard minimum of 17 counts in a TGF (before background subtraction). This helped keep false positive detections out of the first catalog, but also caused a lot of events to be missed [*Gjesteland et al.*, 2012; *Østgaard et al.*, 2015].

Figure 12 shows the distribution of the number of background-subtracted counts in the new catalog used here. The new TGF detection algorithm, which is still being refined, uses true Poisson statistics, as was done by *Gjesteland et al.* [2012] but not *Grefenstette et al.* [2009], but also searches independently for significant excesses over a range of of time scales (from 60 μs to 30 ms). The number of counts per TGF is a continuous rather than discrete variable because the background for each TGF, which is averaged over a long interval nearby and is not an integer, is subtracted. The binning shown is at 0.25 counts, rebinned where necessary to get at least 10 TGFs in each bin before fitting.

In order to find an effective average threshold number of counts, N_1, for inclusion in the data set, we fit the data in Figure 12 to the following function:

$$\frac{dn}{dN} = \begin{cases} P_0 N^{-2.3}\left[\frac{1}{2}\mathrm{erf}\left(\frac{(N-P_1)}{P_2}+1\right)\right] & N < P_4 \\ P_0 N^{-2.3}\left[\frac{1}{2}\mathrm{erf}\left(\frac{(N-P_1)}{P_2}+1\right)\right]\left[e^{\left(-\frac{(N-P_4)}{P_3}\right)}\right] & N \geq P_4 \end{cases} \tag{A10}$$

with P_0 through P_4 being free parameters. This is the expected power law of index 2.3 [*Østgaard et al.*, 2012; *Tierney et al.*, 2013; *Marisaldi et al.*, 2014] with a cutoff in the form of an error function on the low end due to instrumental sensitivity (including variable background) and a steepening on the high end in the form of an exponential due to deadtime at high count rates. The forms of these two cutoffs are empirical, not theoretically motivated. The fit is good, with a χ^2 value of 111 for 124 degrees of freedom. The values of the parameters of the fit and their 1σ errors are: $P_0 = (3.97 \pm 0.12) \times 10^4$, $P_1 = (14.60 \pm 0.20)$, $P_2 = (4.44 \pm 0.19)$, $P_3 = (17.3 \pm 1.5)$, and $P_4 = (30.4 \pm 1.2)$. We compare the fitted function with and without its low-count cutoff to find the effective threshold point N_1 where the same number of TGFs above the threshold are missed as there are TGFs below the threshold picked up. This effective threshold N_1 is 13.625 counts.

References

Abarca, S. F., K. L. Corbosiero, and T. J. Galarneau, An evaluation of the Worldwide Lightning Location Network (WWLLN) using the National Lightning Detection Network (NLDN) as ground truth, *Journal of Geophysical Research (Atmospheres)*, *115*, D18,206, 2010.

Boccippio, D. J., K. L. Cummins, H. J. Christian, and S. J. Goodman, Combined Satellite- and Surface-Based Estimation of the Intracloud Cloud-to-Ground Lightning Ratio over the Continental United States, *Monthly Weather Review*, *129*, 108, 2001.

Briggs, M. S., et al., Terrestrial gamma-ray flashes in the Fermi era: Improved observations and analysis methods, *Journal of Geophysical Research (Space Physics)*, *118*, 3805–3830, 2013.

Carlson, B. E., N. G. Lehtinen, and U. S. Inan, Constraints on terrestrial gamma ray flash production from satellite observation, *Geophys. Res. Let.*, *34*, L08,809, 2007.

Carlson, B. E., T. Gjesteland, and N. Østgaard, Connecting the terrestrial gamma-ray flash source strength and observed fluence distributions, *Journal of Geophysical Research (Space Physics)*, *117*, 1314, 2012.

Celestin, S., and V. P. Pasko, Compton scattering effects on the duration of terrestrial gamma-ray flashes, *Geophys. Res. Let.*, *39*, 2802, 2012.

Celestin, S., W. Xu, and V. P. Pasko, Terrestrial gamma ray flashes with energies up to 100 MeV produced by nonequilibrium acceleration of electrons in lightning, *Journal of Geophysical Research (Space Physics)*, *117*, 5315, 2012.

Celestin, S., W. Xu, and V. P. Pasko, Variability in fluence and spectrum of high-energy photon bursts produced by lightning leaders, *Journal of Geophysical Research (Space Physics)*, *120*, 10, 2015.

Cohen, M. B., U. S. Inan, R. K. Said, and T. Gjestland, Geolocation of terrestrial gamma-ray flash source lightning, *Geophys. Res. Let.*, *37*, L02,801, 2010.

Collier, A. B., T. Gjesteland, and N. ØStgaard, Assessing the power law distribution of TGFs, *Journal of Geophysical Research (Space Physics)*, *116*, 10,320, 2011.

Connaughton, V., et al., Associations between Fermi Gamma-ray Burst Monitor terrestrial gamma ray flashes and sferics from the World Wide Lightning Location Network, *Journal of Geophysical Research (Space Physics)*, *115*, 12,307–+, 2010.

Connaughton, V., et al., Radio signals from electron beams in terrestrial gamma ray flashes, *Journal of Geophysical Research (Space Physics)*, *118*, 2313–2320, 2013.

Cummer, S. A., Y. Zhai, W. Hu, D. M. Smith, L. I. Lopez, and M. A. Stanley, Measurement and implications of the relationship between lightning and terrestrial gamma-ray flashes, *Geophys. Res. Let.*, *32*, L22,804, 2005.

Cummer, S. A., G. Lu, M. S. Briggs, V. Connaughton, S. Xiong, G. J. Fishman, and J. R. Dwyer, The lightning-TGF relationship on microsecond timescales, *Geophys. Res. Let.*, *38*, 14,810, 2011.

Cummer, S. A., M. S. Briggs, J. R. Dwyer, S. Xiong, V. Connaughton, G. J. Fishman, G. Lu, F. Lyu, and R. Solanki, The source altitude, electric current, and intrinsic brightness of terrestrial gamma ray flashes, *Geophys. Res. Let.*, *41*, 8586–8593, 2014.

Cummer, S. A., F. Lyu, M. S. Briggs, G. Fitzpatrick, O. J. Roberts, and J. R. Dwyer, Lightning leader altitude progression in terrestrial gamma-ray flashes, *Geophys. Res. Lett.,* , *42*, 7792–7798, 2015.

Dwyer, J. R., and S. A. Cummer, Radio emissions from terrestrial gamma-ray flashes, *Journal of Geophysical Research (Space Physics)*, *118*, 3769–3790, 2013.

Dwyer, J. R., and D. M. Smith, A comparison between Monte Carlo simulations of runaway breakdown and terrestrial gamma-ray flash observations, *Geophys. Res. Let.*, *32*, L08,811, 2005.

Dwyer, J. R., D. M. Smith, M. A. Uman, Z. Saleh, B. Grefenstette, B. Hazelton, and H. K. Rassoul, Estimation of the fluence of high-energy electron bursts produced by thunderclouds and the resulting radiation doses received in aircraft, *J. Geophys. Res.*, *115*, D09,206, 2010.

Fuschino, F., et al., High spatial resolution correlation of AGILE TGFs and global lightning activity above the equatorial belt, *Geophys. Res. Let.*, *38*, L14,806, 2011.

Gjesteland, T., N. Østgaard, P. H. Connell, J. Stadsnes, and G. J. Fishman, Effects of dead time losses on terrestrial gamma ray flash measurements with the Burst and Transient Source Experiment, *Journal of Geophysical Research (Space Physics)*, *115*, 0, 2010.

Gjesteland, T., N. Østgaard, A. B. Collier, B. E. Carlson, M. B. Cohen, and N. G. Lehtinen, Confining the angular distribution of terrestrial gamma ray flash emission, *Journal of Geophysical Research (Space Physics)*, *116*, 11,313, 2011.

Gjesteland, T., N. Østgaard, A. B. Collier, B. E. Carlson, C. Eyles, and D. M. Smith, A new method reveals more TGFs in the RHESSI data, *Geophys. Res. Let.*, *39*, 5102, 2012.

Gjesteland, T., N. Østgaard, R. Nisi, A. Collier, G. Lu, S. Cummer, and D. Smith, Twelve Years of RHESSI TGFs - The second RHESSI TGF catalog., in *EGU General Assembly Conference Abstracts*, vol. 16 of *EGU General Assembly Conference Abstracts*, p. 14125, 2014.

Gjesteland, T., et al., Observation of intrinsically bright terrestrial gamma ray flashes from the mediterranean basin, *Journal of Geophysical Research: Atmospheres*, *120*, 12,143–12,156, 2015, 2015JD023704.

Grefenstette, B., D. Smith, B. Hazelton, and L. Lopez, First RHESSI terrestrial gamma-ray flash catalog, *J. Geophys. Res.*, *114*, A02,314, 2009.

Grefenstette, B. W., D. M. Smith, J. R. Dwyer, and G. J. Fishman, Time evolution of terrestrial gamma-ray flashes, *Geophys. Res. Let.*, *35*, L06,802, 2007.

Hansen, R. S., N. ØStgaard, T. Gjesteland, and B. Carlson, How simulated fluence of photons from terrestrial gamma ray flashes at aircraft and balloon altitudes depends on initial parameters, *Journal of Geophysical Research (Space Physics)*, *118*, 2333–2339, 2013.

Hazelton, B., B. Grefenstette, D. Smith, J. Dwyer, X.-M. Shao, S. Cummer, T. Chronis, E. Lay, and R. Holzworth, Spectral dependence of terrestrial gamma-ray flashes on source distance, *Geophys. Res. Let.*, *36*, L01,108, 2009.

Hazelton, B. J. C., Statistical studies and modeling of RHESSI terrestrial gamma-ray flashes, Ph.D. thesis, University of California, Santa Cruz, 2009.

Humphreys, W., *Physics of Air, 3rd ed*, Dover Publications, 1964.

Hutchins, M. L., R. H. Holzworth, J. B. Brundell, and C. J. Rodger, Relative detection efficiency of the World Wide Lightning Location Network, *Radio Science*, *47*, 6005, 2012a.

Hutchins, M. L., R. H. Holzworth, C. J. Rodger, S. Heckman, and J. B. Brundell, WWLLN Absolute Detection Efficiencies and the Global Lightning Source Function, retrieved from http://staff.washington.edu/mlhutch/pdf/Hutchins_EGU_2012.pdf on 17 October 2014, in *EGU General Assembly Conference Abstracts*, edited by A. Abbasi and N. Giesen, vol. 14 of *EGU General Assembly Conference Abstracts*, p. 12917, 2012b.

Inan, U., and N. Lehtinen, Production of terrestrial gamma-ray flashes by an electromagnetic pulse from a lightning return stroke, *Geophys. Res. Let.*, *32*, L19,818, 2005.

Jacobson, A. R., R. H. Holzworth, J. Harlin, R. L. Dowden, and E. H. Lay, Performance assessment of the world wide lightning location network (wwlln) using the los alamos sferic array (lasa) as ground truth, *J. Atmos. Oceanic Technol.*, *23*, 1082–1092, 2006.

Kelley, N., D. Smith, J. Dwyer, M. Splitt, R. Holzworth, P. Buzbee, A. Infanger, and S. Lazarus, The brightest TGF ever observed? - New results from the RHESSI satellite, in *EGU General Assembly Conference Abstracts*, vol. 17 of *EGU General Assembly Conference Abstracts*, p. 4212, 2015.

Lay, E. H., R. H. Holzworth, C. J. Rodger, J. N. Thomas, O. Pinto, and R. L. Dowden, WWLL global lightning detection system: Regional validation study in Brazil, *Geophys. Res. Let.*, *31*, 3102, 2004.

Lehtinen, N., T. Bell, and U. Inan, Monte carlo simulation of runaway mev electron breakdown with application to red sprites and terrestrial gamma ray flashes, *J. Geophys. Res.*, *104*, 24,699–24,712, 1999.

Lu, G., S. A. Cummer, J. Li, F. Han, D. M. Smith, and B. W. Grefenstette, Characteristics of broadband lightning emissions associated with terrestrial gamma ray flashes, *Journal of Geophysical Research (Space Physics)*, *116*, A03,316, 2011.

Lu, G., et al., Lightning mapping observation of a terrestrial gamma-ray flash, *Geophys. Res. Let.*, *37*, L11,806, 2010.

Lyu, F., S. A. Cummer, and L. McTague, Insights into high peak current in-cloud lightning events during thunderstorms, *Geophys. Res. Lett.,* , *42*, 6836–6843, 2015.

Marisaldi, M., et al., Properties of terrestrial gamma ray flashes detected by AGILE MCAL below 30 MeV, *Journal of Geophysical Research (Space Physics)*, *119*, 1337–1355, 2014.

Marisaldi, M., et al., Enhanced detection of terrestrial gamma-ray flashes by AGILE, *Geophys. Res. Let.*, *42*, 9481–9487, 2015.

McTague, L. E., S. A. Cummer, M. S. Briggs, V. Connaughton, M. Stanbro, and G. Fitzpatrick, A lightning-based search for nearby observationally dim terrestrial gamma ray flashes, *Journal of Geophysical Research (Atmospheres)*, *120*, 12, 2015.

Nisi, R. S., N. Østgaard, T. Gjesteland, and A. B. Collier, An altitude and distance correction to the source fluence distribution of TGFs, *Journal of Geophysical Research (Space Physics)*, *119*, 8698–8704, 2014.

Omar, K., S. Xiong, M. S. Briggs, and S. Heckman, Characterizing the TGF-Lightning Relationship Using ENTLN, *AGU Fall Meeting Abstracts*, 2014.

Østgaard, N., T. Gjesteland, J. Stadnses, P. H. Connell, and B. Carlson, Production altitude and time delays of the terrestrial gamma flashes: Revisiting the burst and transient source experiment spectra, *J. Geophys. Res.*, *113*, 2008.

Østgaard, N., T. Gjesteland, R. S. Hansen, A. B. Collier, and B. Carlson, The true fluence distribution of terrestrial gamma flashes at satellite altitude, *Journal of Geophysical Research (Space Physics)*, *117*, 3327, 2012.

Østgaard, N., K. H. Albrecthsen, T. Gjesteland, and A. Collier, A new population of terrestrial gamma-ray flashes in the RHESSI data, *Geophys. Res. Let.*, *42*, 10, 2015.

Price, C., and D. Rind, A Simple lightning parameterization for calculating global lightning distributions, *J. Geophys. Res.*, *97*, 9919–9933, 1992.

Rodger, C. J., J. B. Brundell, R. H. Holzworth, E. H. Lay, and R. L. Dowden, Improvements in the wwlln network: Growing detection efficiencies for "big lightning" events, *paper presented at the Workshop on Coupling of Thunderstorms and Lightning Discharges to Near-Earth Space, Corte, France*, 2008.

Roussel-Dupré, R., and A. Gurevich, On runaway breakdown and upward propagating discharges, *J. Geophys. Res.*, *101*, 2297–2311, 1996.

Saleh, Z., et al., Properties of the X-ray emission from rocket-triggered lightning as measured by the Thunderstorm Energetic Radiation Array (TERA), *Journal of Geophysical*

Research (Atmospheres), *114*, 17,210, 2009.

Shao, X.-M., T. D. Hamlin, and D. M. Smith, A closer examination of terrestrial gamma-ray flash-related lightning processes, *J. Geophys. Res.*, *115*, A00E30, 2010.

Smith, D. M., B. J. Hazelton, B. W. Grefenstette, J. R. Dwyer, R. J. Holzworth, and E. H. Lay, Terrestrial gamma ray flashes correlated to storm phase and tropopause height, *J. Geophys. Res.*, *115*, A00E49, 2010.

Smith, D. M., P. Buzbee, S. Aron-Dine, N. A. Kelley, R. H. Holzworth, II, M. L. Hutchins, and J. R. Dwyer, Constraining faint terrestrial gamma-ray flashes with stacking analyses, *AGU Fall Meeting Abstracts*, 2014.

Smith, D. M., et al., The RHESSI Spectrometer, *Solar Phys.*, *210*, 33–60, 2002.

Smith, D. M., et al., The rarity of terrestrial gamma-ray flashes, *Geophys. Res. Let.*, *38*, L08,807, 2011.

Stanley, M. A., X. Shao, D. M. Smith, L. Lopez, M. Pongratz, J. Harlin, M. Stock, and A. Regan, A link between terrestrial gamma-ray flashes and intracloud lightning discharges, *Geophys. Res. Let.*, *33*, L06,803, 2006.

Tierney, D., et al., Fluence distribution of terrestrial gamma ray flashes observed by the Fermi Gamma-ray Burst Monitor, *Journal of Geophysical Research (Space Physics)*, *118*, 6644–6650, 2013.

Ushio, T., S. J. Heckman, D. J. Boccippio, H. J. Christian, and Z.-I. Kawasaki, A survey of thunderstorm flash rates compared to cloud top height using TRMM satellite data, *J. Geophys. Res.*, *106*, 24, 2001.

Table 2. Number of counts at the spectral break and percent of lightning creating TGFs of any intensity

Model	Counts at break (N_0), group I	% TGFs group I	Counts at break (N_0), group I+II	% TGFs group I+II
$\lambda = 2.3$, λ_0 =cutoff	4.32	0.23 / 0.23 [a]	2.56	0.44 / 0.44
$\lambda = 2.3$, $\lambda_0 = -1$	5.88	0.25 / 0.25	3.49	0.48 / 0.48
$\lambda = 2.3$, $\lambda_0 = 0$	6.82	0.28 / 0.28	4.04	0.56 / 0.56
$\lambda = 2.3$, $\lambda_0 = 0.5$	7.85	0.37 / 0.36	4.66	0.72 / 0.72
$\lambda = 2.3$, $\lambda_0 = 0.9$	9.56	1.11 / 0.68	5.67	2.18 / 1.30
$\lambda = 2.3$, $\lambda_0 = 0.99$	10.18	9.56 / 0.88	6.04	18.84 / 1.65
Østgaard (see text)	2.20	0.29	0.37	1.11

[a] The percentage before the slash includes all TGFs in the distribution down to zero luminosity; the percentage after the slash includes only those $> 10^{-4}$ of a threshold TGF (1.36×10^{-3} *RHESSI* counts).

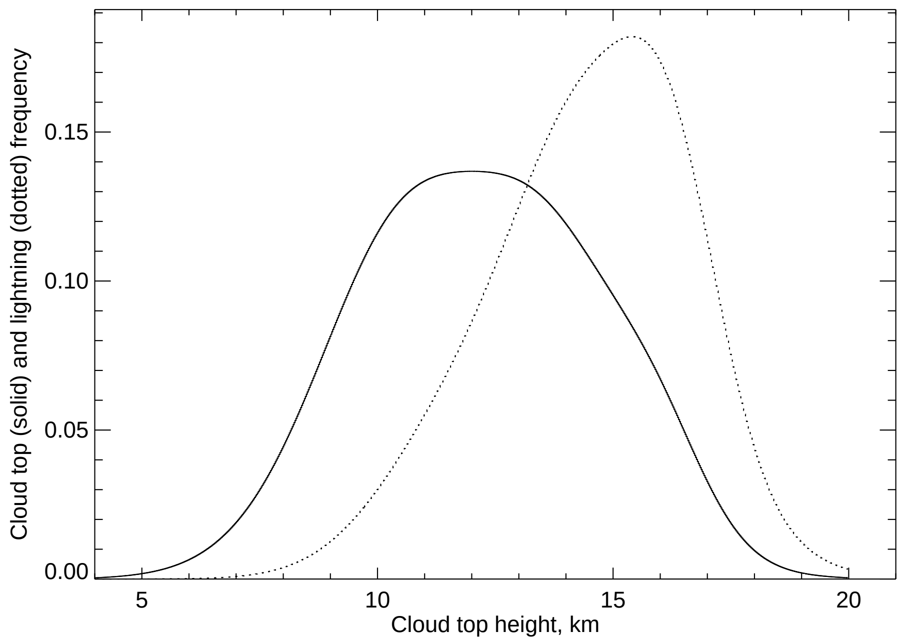

Figure 1. Solid curve: differential distribution of cloud top height for tropical thunderstorms over land, adapted from *Ushio et al.* [2001]. Dashed curve: the same, multiplied by the flash rate prescription of *Price and Rind* [1992] to show the lack of significant extra lightning in low-altitude storms.

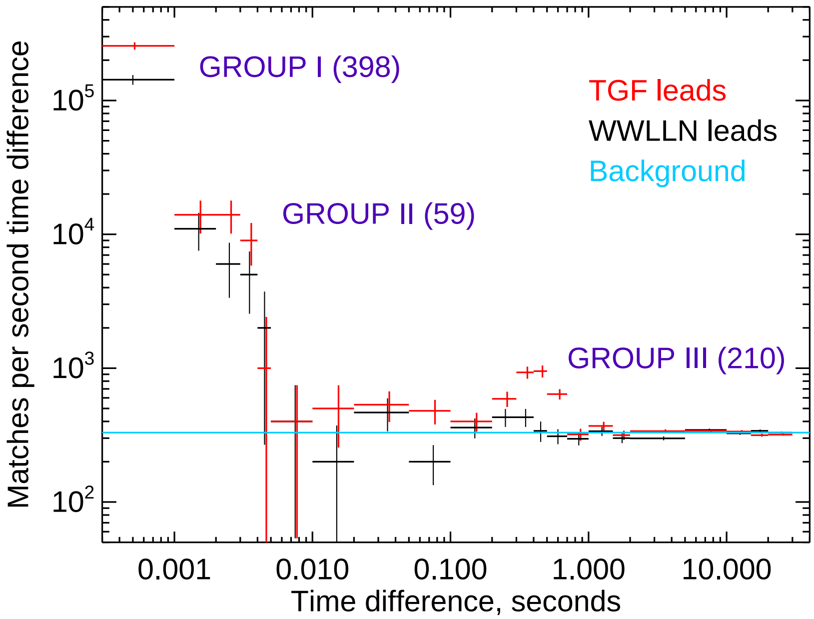

Figure 2. Histogram of relative time delays between a TGF in the catalog used here and a WWLLN sferic within 700 km. The background level due to chance coincidences is shown in blue-green. The three groups of relative timing are from -2 to +2 ms time difference (group I), between 2 and 10 ms in absolute time difference (group II), and with the TGF leading WWLLN by 200–800 ms (group III). The number in parentheses by each group is the excess above the background level, which is measured using time differences of 5–30 seconds, where no real matches are expected.

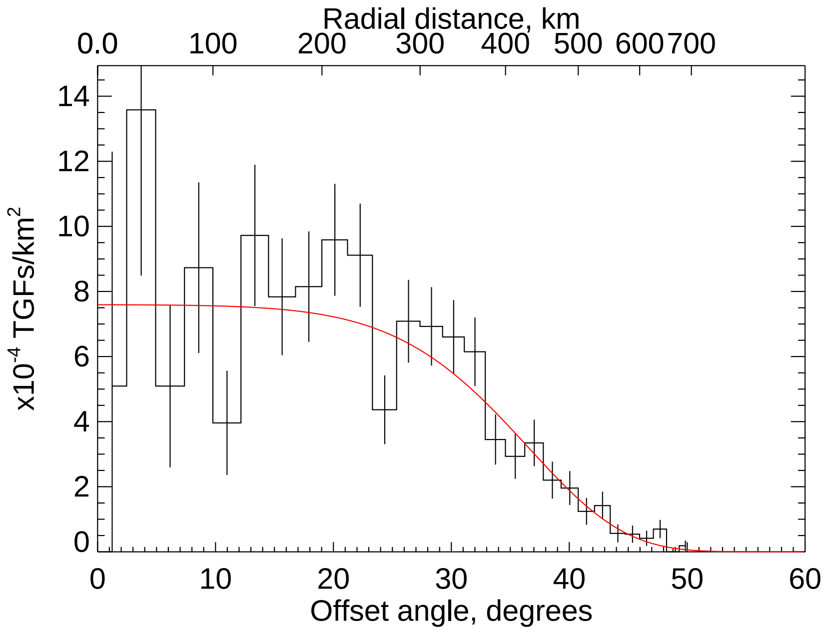

Figure 3. Surface density of TGFs as a function of radial distance from the *RHESSI* subsatellite point (upper x axis), including 477 events from 2004 to 2012 with a match to a WWLLN discharge within 5 ms and 1000 km. The lower x axis represents the angle between an upward ray at the position of the WWLLN discharge and a ray directed from the WWLLN discharge point to *RHESSI*. The fit in red is to an error function (see text).

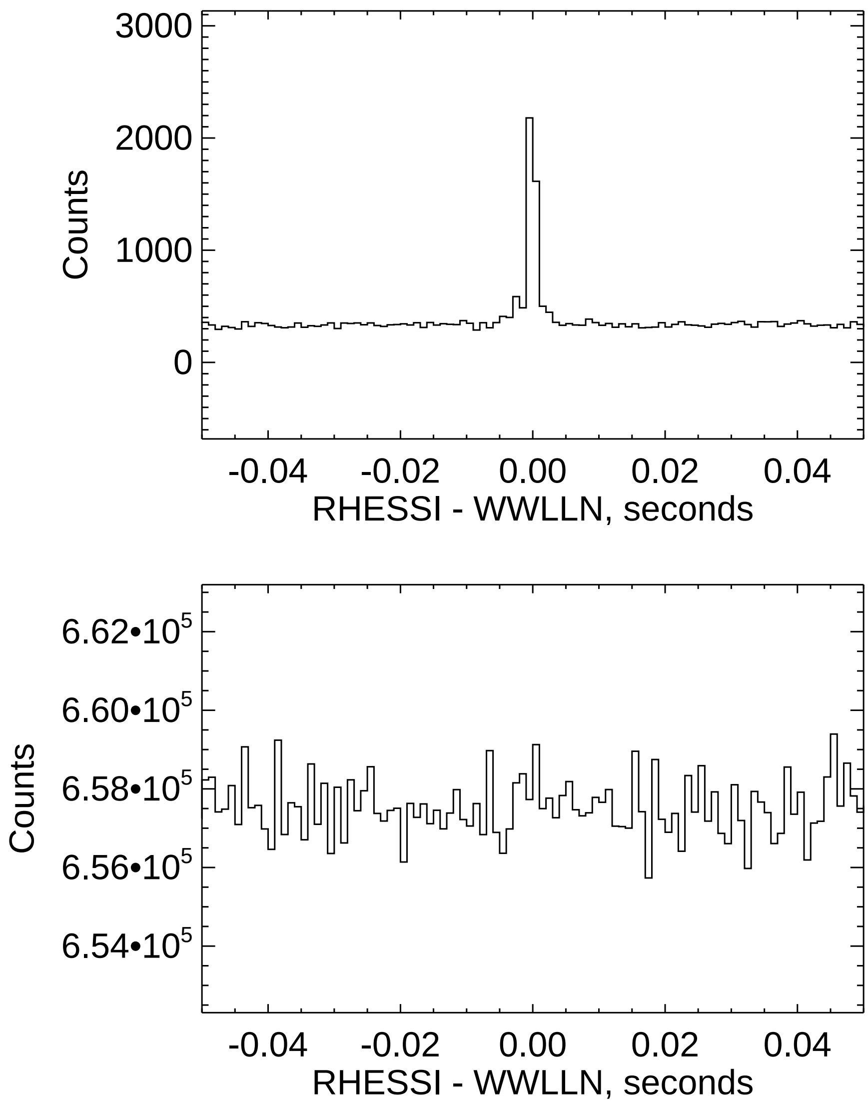

Figure 4. Stacked histograms of gamma-ray arrival times centered on the expected arrival time of a signal from each WWLLN discharge, with 1 ms binning. Top: summed over the 216 discharges within 10 ms and 300 km of an independently detected *RHESSI* TGF. Bottom: summed over the 432,342 discharges within 300 km of *RHESSI*'s subsatellite point with no known TGF within 1.25 s.

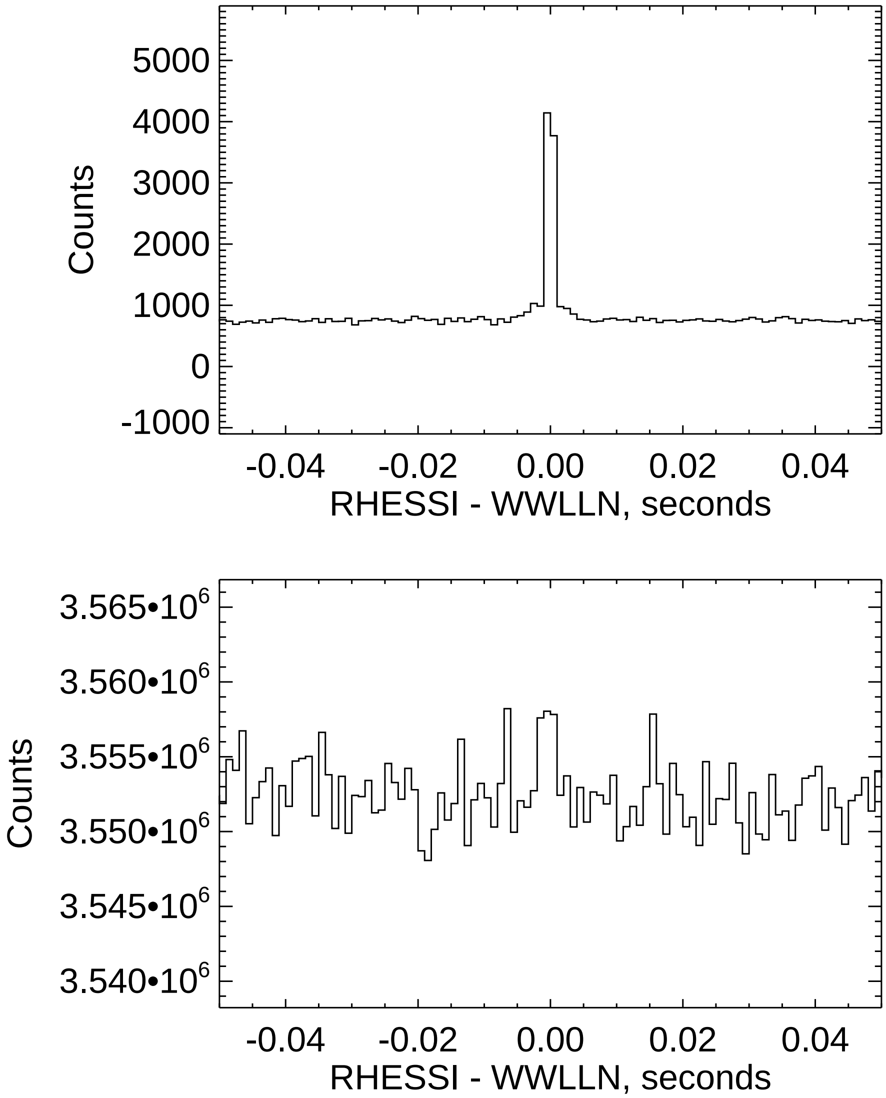

Figure 5. As Figure 4 for a radial distance range of 0–700 km, with 461 discharges included in the upper panel and 2,338,292 in the lower.

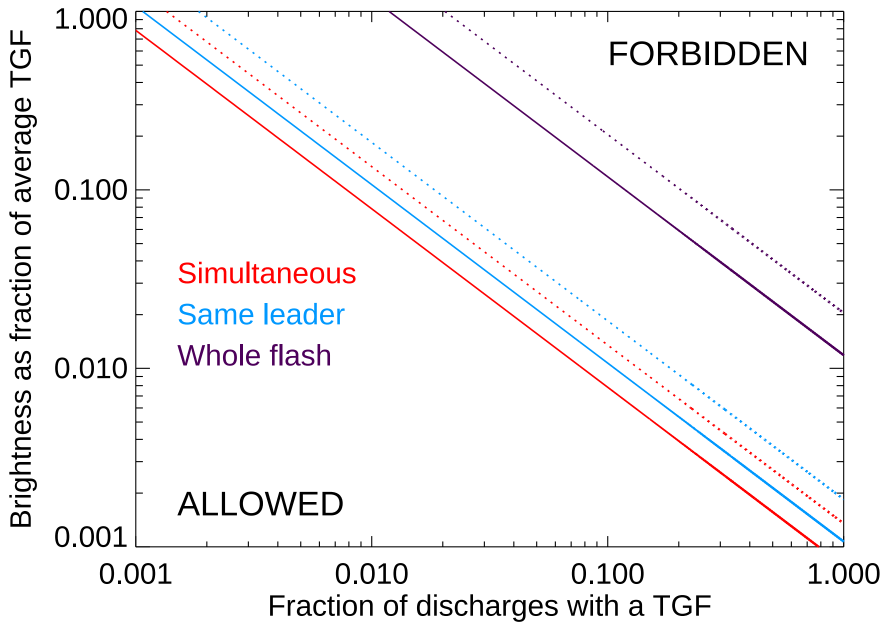

Figure 6. Upper limits (95% confidence) on the average allowed gamma-ray brightness of WWLLN discharges from 0–300 km expressed as a function of the fraction of such discharges assumed to contribute. Red: gammas averaged over ±2 ms of the WWLLN event ("group I" of Figure 2). Blue: gammas averaged over ±10 ms of the WWLLN event ("groups I+II" of Figure 2). Purple: gammas averaged over all time differences that generally relate known TGFs with WWLLN events ("groups I+II+III" or ±10 ms plus 200–800 ms with the gammas leading). Solid lines assume all WWLLN events are of interest. Dashed lines assume only 58% of WWLLN events (the approximate number that are +IC lightning) are of interest as potential gamma-ray producers.

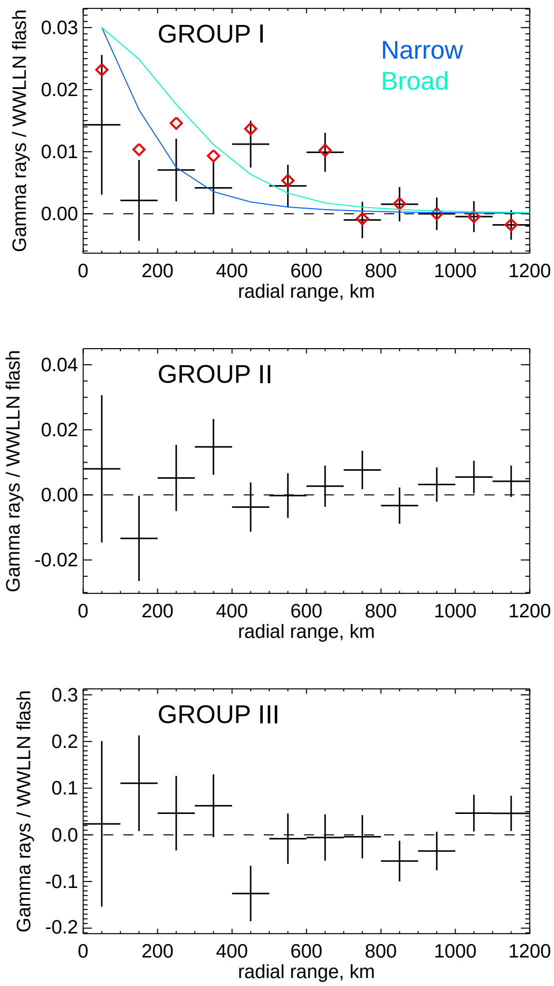

Figure 7. *RHESSI* counts per WWLLN flash as a function of the ground distance between the WWLLN flash position and the *RHESSI* subsatellite point. Top: Gammas summed within ±2 ms of the WWLLN event. Middle: gammas summed between 2 and 10 ms in either direction of the WWLLN event. Bottom: Gammas summed between 200 and 800 ms before the WWLLN event. In the top panel, the red points include the counts from the known (independently detected) TGFs as well as the rest of the WWLLN flashes. The blue curves represent, with arbitrary normalization, the expected falloff from a TGF produced at 13 km altitude with the narrow and broad angular distributions described in the text.

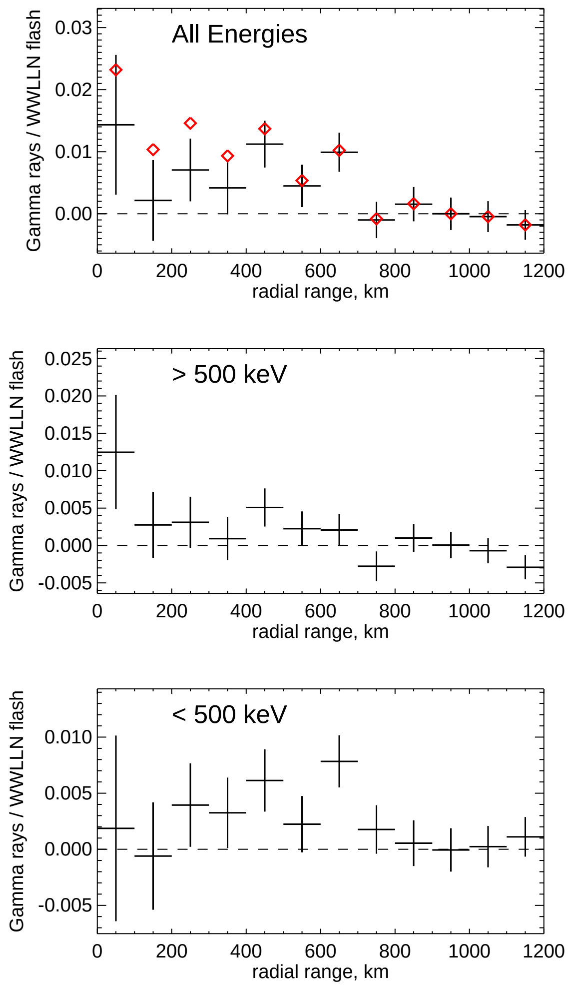

Figure 8. As Figure 7 but each panel includes only "group I" *RHESSI* counts (within ±2 ms of the WWLLN event), with the middle and bottom panels containing only counts > 500 keV and < 500 keV, respectively.

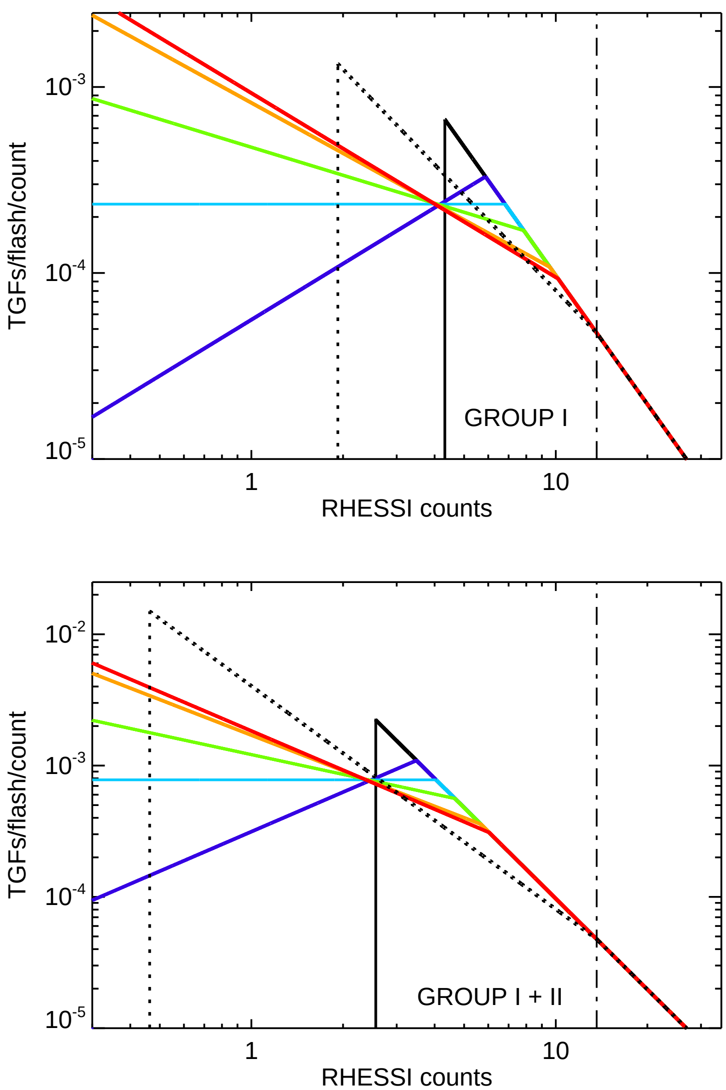

Figure 9. Broken power law TGF differential intensity distributions giving the known rate of TGFs above the mean *RHESSI* detection threshold, with differential power law index 2.3, and an integral of counts below that threshold equal to the 95% confidence upper limit for 0–300 km from the stacking analysis. Top: *RHESSI* data summed within ±2 ms of the WWLLN event only. Bottom: *RHESSI* data summed within ±10 ms of the WWLLN event. The colors black, purple, blue, green, orange, and red represent, in that order, the first six rows of Table 2. The dotted line is the hardening index suggested by *Østgaard et al.* [2012] (see text) shown in the last row of Table 2.

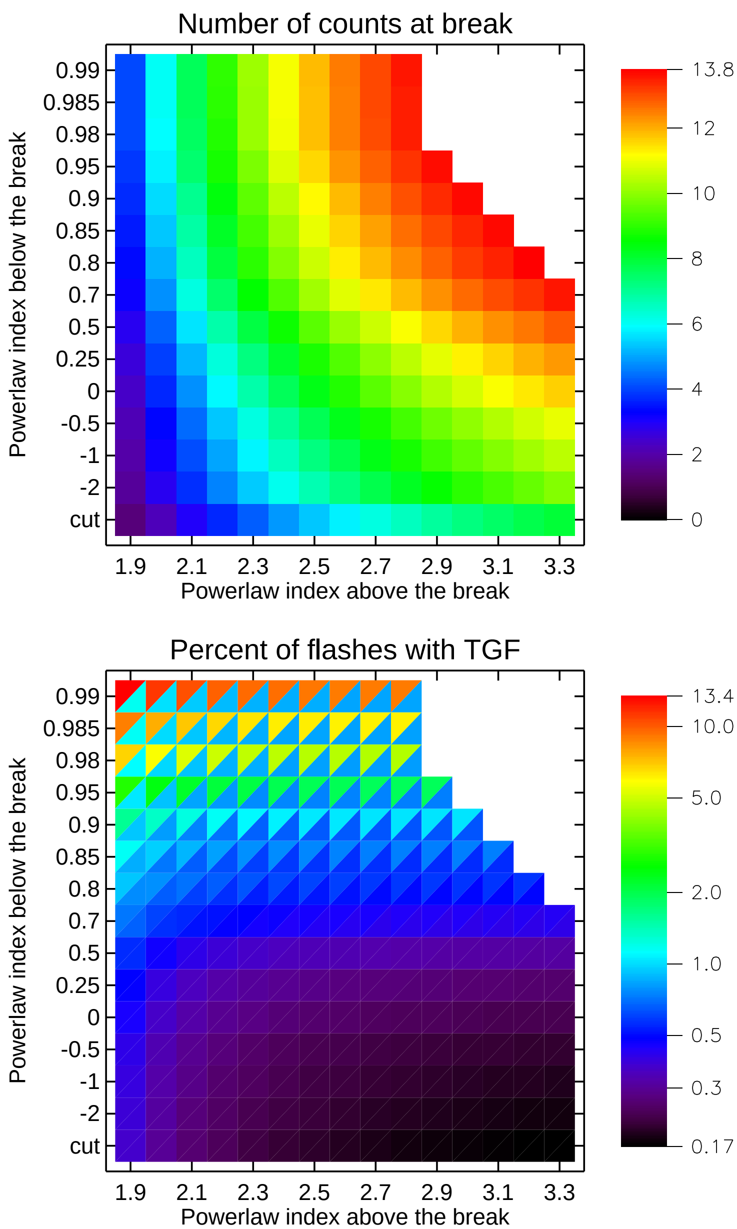

Figure 10. Number of *RHESSI* counts at the power-law break (top) and percentage of WWLLN flashes encompassed by the entire distribution (bottom), consistent with the 95% upper limit on *RHESSI* counts simultaneous with WWLLN within ±2 ms ("group I"), for the 0–300 km radial distance range, as a function of all power law indices explored above (λ) and below (λ_0) the break. In the bottom panel, the color in the upper left of each box represents all TGFs in the distribution, no matter how faint, while the color in the lower right represents only those TGFs above 1.36×10^{-3} *RHESSI* counts (see text). In the range not filled in, the number of counts at the break exceeds the effective threshold for known individual TGFs, 13.625 counts.

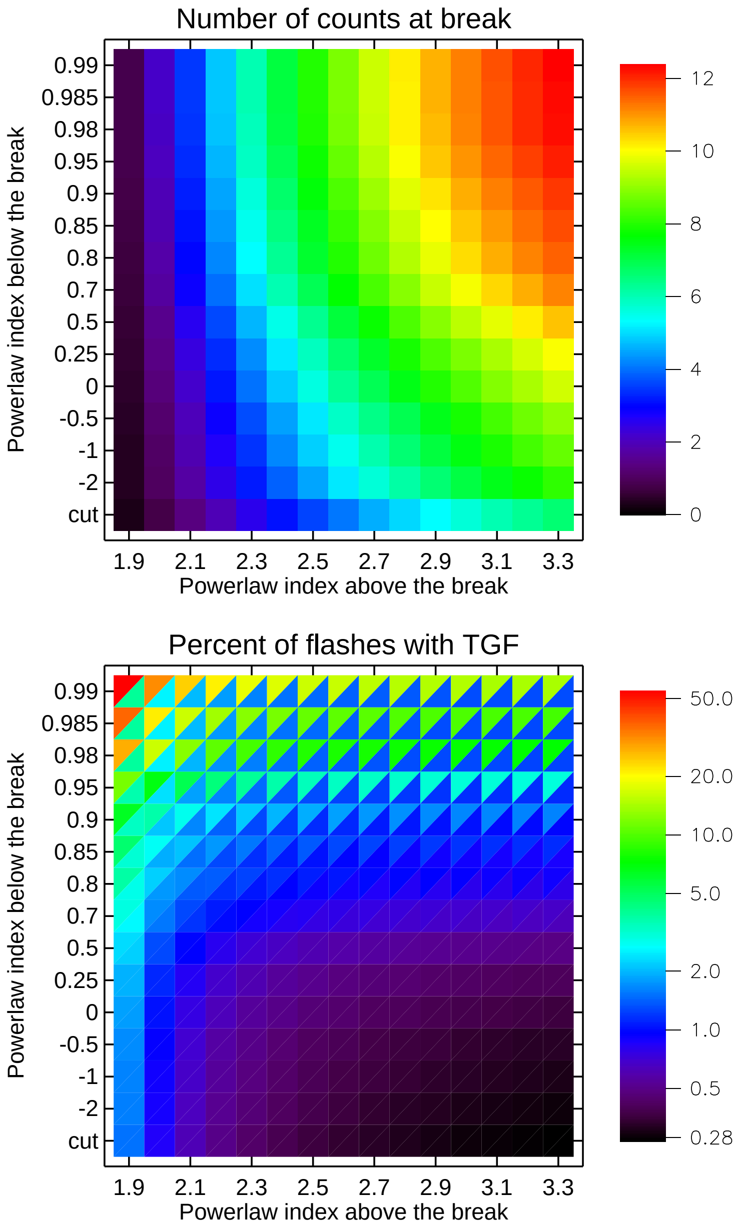

Figure 11. As Figure 10, but for all *RHESSI* counts within ±10 ms (“groups I+II”).

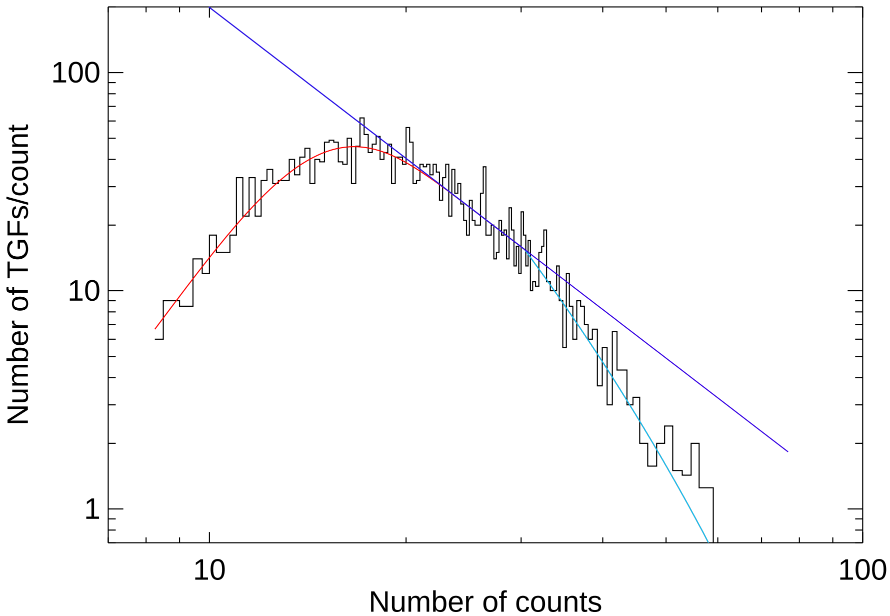

Figure 12. Differential distribution of the number of *RHESSI* counts in the sample of known TGFs from the current algorithm. The data were fit with a model consisting of a power law of index $\lambda = 2.3$ (purple curve) with cutoffs at the low end (red) to represent the sensitivity limit and the high end (blue) to represent the presumed effect of dead time.